Check for updates

Cytoskeleton
SPECIAL ISSUE Cytoskeletal Methods

WILEY
CYTOSKELETON

REVIEW ARTICLE OPEN ACCESS

Cytoskeletal Dynamics: Advances in Computational Modeling and Simulations

Remi Sondaz[1,2] | Dheeraj Prakaash[1] | Tamara Bidone[1,2,3,4]

[1]Scientific Computing and Imaging Institute, University of Utah, Salt Lake City, Utah, USA | [2]Department of Biomedical Engineering, University of Utah, Salt Lake City, Utah, USA | [3]Department of Molecular Pharmaceutics, University of Utah, Salt Lake City, Utah, USA | [4]Department of Biochemistry, University of Utah, Salt Lake City, Utah, USA

Correspondence: Tamara Bidone (tamarabidone@sci.utah.edu)

Received: 5 January 2026 | **Revised:** 16 October 2026 | **Accepted:** 5 November 2026

ABSTRACT

The cytoskeleton is a highly dynamic network that regulates cell behavior across multiple spatial and temporal scales, from atomic interactions to assembly and disassembly of large macromolecular complexes. Capturing this complexity computationally requires approaches that balance molecular detail with access to biologically relevant timescales. Recent advances in all-atom, coarse-grained, and mesoscale modeling have significantly expanded the range of cytoskeletal phenomena that can be explored, though challenges remain in integrating these methods across scales. This review highlights recent progress in all-atom, coarse-grained, and mesoscale computational approaches for studying cytoskeletal dynamics. All-atom molecular dynamics simulations, enabled by improved force fields, GPU acceleration, and enhanced sampling techniques, now resolve conformational transitions and protein–protein interfaces in cytoskeletal proteins. Coarse-grained and multiscale frameworks translate atomistic energetics into kinetic parameters, enabling simulations of elongation and of cytoskeletal polymers. At larger scales, simulations of cytoskeletal networks and adhesion complexes capture cell contractility, spindle assembly, force transmission and their interplay with the extracellular matrix. Together, these approaches reveal how molecular-scale interactions and stochastic events that drive kinetics and state transitions cooperate to shape cytoskeletal organization and mechanics across scales.

1 | Introduction

The cytoskeleton is a dynamic network of biological polymers and crosslinking proteins that provides structural support, organizes the cytoplasm, and governs cell shape. Actin filaments and microtubules serve as primary structural elements that enable cells to execute these essential processes (Dogterom and Koenderink 2019; Fletcher and Mullins 2010; Parsons et al. 2010; Bezanilla et al. 2015). Microtubules (MTs) are cylindrical polymers of $\alpha\beta$-tubulin dimers that transition between phases of polymerization/growth and depolymerization/shrinking, a behavior called "dynamic instability". Microtubules' dynamic instability enables cells to execute both mechanical and organizational processes, such as the partitioning of chromosomes during cell division, the transport of organelles and the maintenance of cell polarity (Desai and Mitchison 1997; Gardner et al. 2013). Actin filaments (F-actins) are polar, semi-flexible polymers composed of globular subunits (G-actin) organized into a double helix. F-actins form a dynamic, supportive meshwork that generate mechanical forces for contractility and motility (Spiliotis and Nakos 2021). These forces are transmitted to the extracellular environment via adhesions (Blanchoin et al. 2014; Wehrle-Haller and Imhof 2003). The activities of F-actin, MTs, and adhesion complexes are heavily coordinated (Wehrle-Haller and Imhof 2003) through proteins that interact with one or both filaments, including MT-associated and

Remi Sondaz and Dheeraj Prakaash should be considered joint first authors.

This is an open access article under the terms of the Creative Commons Attribution License, which permits use, distribution and reproduction in any medium, provided the original work is properly cited.

© 2026 The Author(s). *Cytoskeleton* published by Wiley Periodicals LLC.

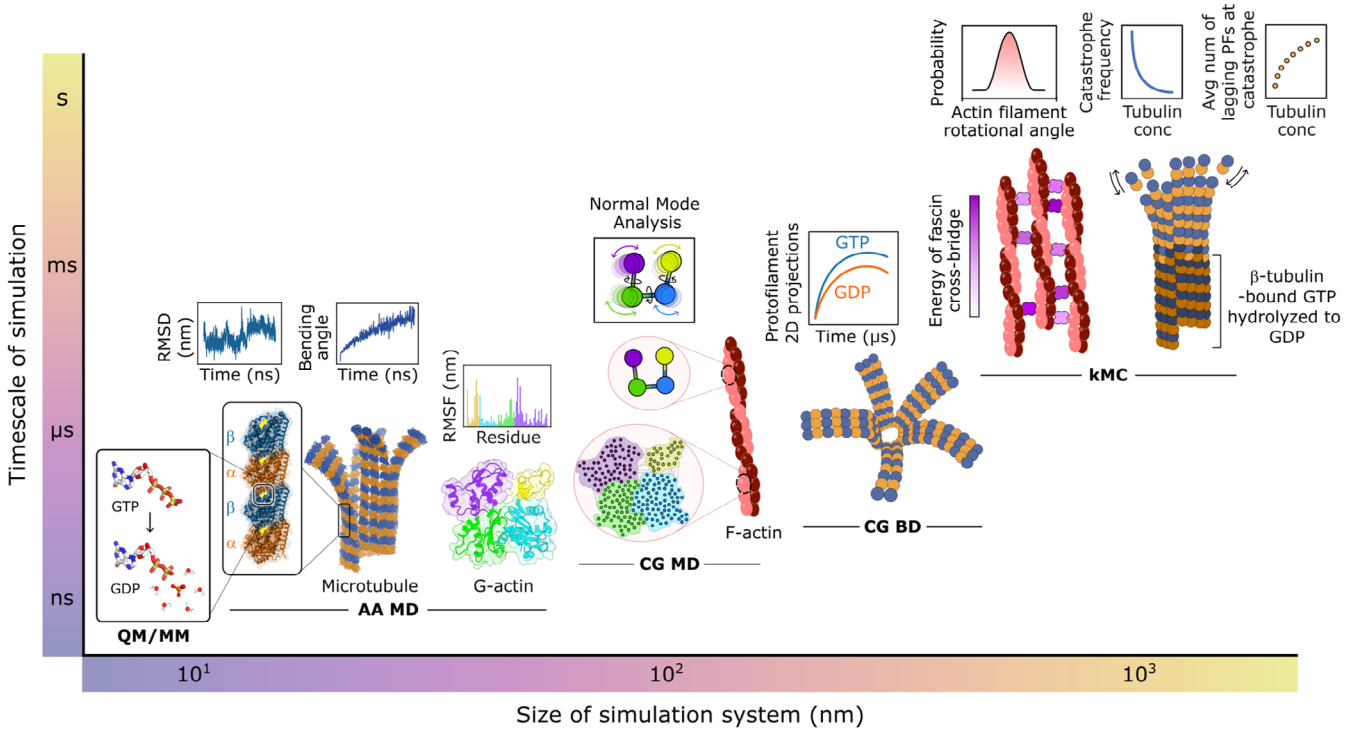

FIGURE 1 | Simulation methodologies to study cytoskeletal dynamics from high-resolution to low-resolution systems. Higher resolution systems are simulated using hybrid quantum mechanics and molecular mechanics (QM/MM), followed by all-atom molecular dynamics (AA MD) simulations. Relatively lower resolution simulation systems are studied using coarse-graining (CG) techniques combined with MD or Brownian dynamics (BD) simulations. Martini forcefield-based simulations (Marrink et al. 2007; Souza et al. 2021) involve a high-resolution ~4:1 CG mapping, explicit solvent particles, and follow CG MD principles, lying in the spatiotemporal space between AA MD and other CG MD methods. CG BD methods treat solvent implicitly. Simulation systems of the largest size and least resolution have employed kinetic Monte Carlo (kMC) algorithms. For each resolution, simulation systems modeled in previous studies are schematically represented along with examples of analyses. The individual plots/colormap displayed for each simulation system are intended to only represent a type of analysis performed for that simulation system, and thus do not show actual data or numerical axis labels. Schematics of simulation systems are inspired by/based on previous studies as follows: QM/MM (Beckett and Voth 2023), AA MD of microtubule (Wu et al. 2025; Hemmat and Odde 2021) and GTP-actin (Deriu et al. 2011), CG MD of F-actin (Deriu et al. 2011; Harker et al. 2019; Chu and Voth 2006), CG BD of microtubule (Skora et al. 2025), kMC of actin filament bundles (Gong et al. 2025) and MTs (Alexandrova et al. 2022).

actin-binding proteins, molecular motors, signaling proteins, and crosslinkers. For example, MAP1, MAP2, MAP4, and Tau-family proteins bridge F-actin and MTs closely via motifs in their intrinsically disordered regions (Mohan and John 2015; Cabrales Fontela et al. 2017; Al-Bassam et al. 2002; Shigematsu et al. 2018). Proteins like the spectraplakin family (e.g., MACF) connect them over larger distances using structured domains (Suozzi et al. 2012). Furthermore, both filaments interact with adhesion complexes (Wehrle-Haller and Imhof 2003; Stehbens and Wittmann 2012). These coordinated functions emerge from molecular interactions that span length scales from individual protein subunits to supramolecular assemblies and cellular networks.

As cytoskeletal polymers and crosslinking proteins operate across a broad range of spatial and temporal scales, computational modeling has become essential to complement experimental approaches. Over the past several decades, all-atom (AA) (Nasedkin et al. 2021; Havelka et al. 2017; Wu et al. 2025), coarse-grained (CG) (Chu and Voth 2005; Skora et al. 2025; Xue et al. 2026; Deriu et al. 2012; Shamloo and Mehrafrooz 2018; Sept and MacKintosh 2010), and mesoscale modeling approaches (Gudimchuk et al. 2020; Hemmat and Odde 2021; Alexandrova et al. 2022; Li et al. 2018) have enabled quantitative investigation of cytoskeletal polymers and crosslinking proteins (Figure 1). AA molecular dynamics (MD) simulations explicitly represent atomic interactions and provide insight into residue-level fluctuations, but are limited to lengths on the order of tens or hundreds of nanometers. CG models reduce molecular complexity by grouping atoms into effective interaction sites, extending simulations to larger assemblies and longer timescales. Together, AA and CG simulations connect static structural data from experimental techniques such as cryo-electron microscopy (cryo-EM) and crystallography to dynamic molecular behavior. Mesoscale frameworks further simplify molecular and macromolecular details to capture emergent behaviors such as network remodeling, force transmission, and cell–matrix coupling at length scales of several micrometers and timescales of minutes. Together, these approaches enable the investigation of cytoskeletal mechanisms that are inaccessible experimentally.

Synthesizing these methodological perspectives, this review focuses on recent computational advances applied to the study of F-actin, MTs, and actin–adhesion systems. To guide the reader through this synthesis, we first discuss AA MD simulations of cytoskeletal filaments and discuss approaches for enhancing

19493592, 0, Downloaded from https://onlinelibrary.wiley.com/doi/10.1002/cm.70221, Wiley Online Library on [25/11/2026]. See the Terms and Conditions (https://onlinelibrary.wiley.com/terms-and-conditions) on Wiley Online Library for rules of use; OA articles are governed by the applicable Creative Commons License

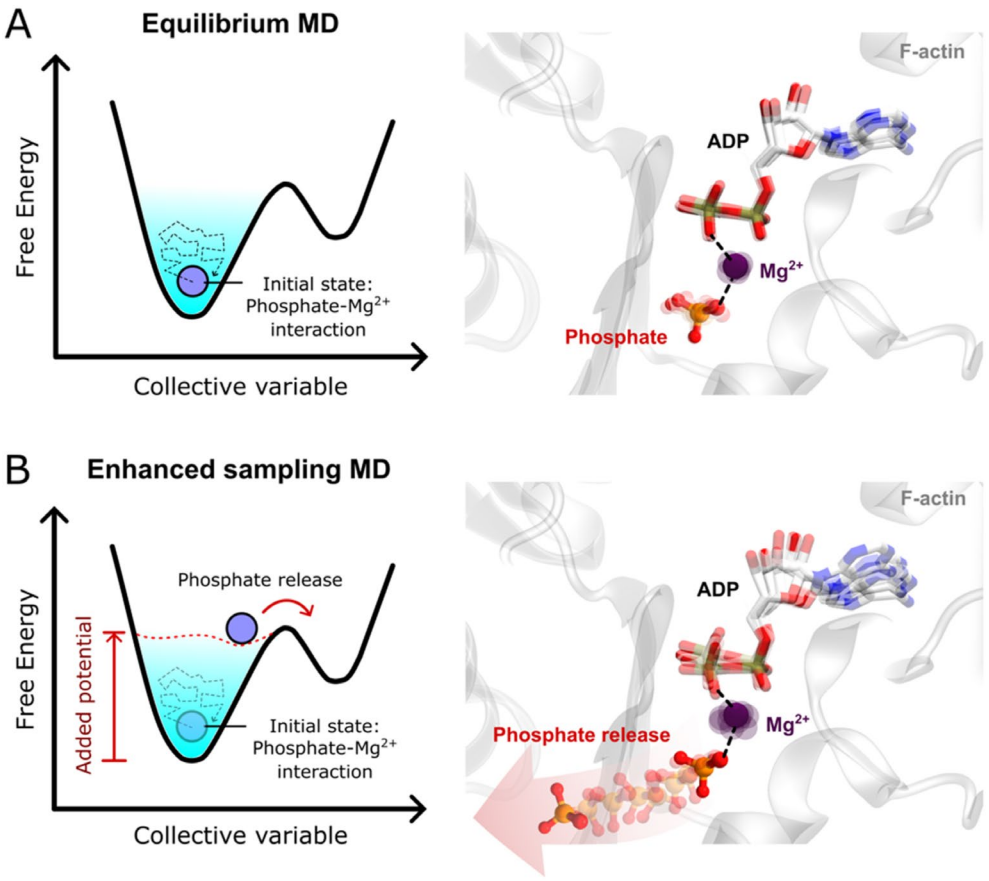

FIGURE 2 | Differentiating the capability of equilibrium MD and enhanced sampling MD simulations. The example simulation system considered here is based on a previous study (Wang et al. 2024). (A) In equilibrium AA MD simulations, a phosphate ion electrostatically interacting with a Mg^{2+} cation within a monomer of F-actin encounters an energy barrier to dissociate. Therefore, this dissociation event and exit pathway of the phosphate ion may not be sampled unless simulated for longer at a significantly higher computational cost. (B) In enhanced sampling MD simulations, an external potential is applied either to pull the phosphate ion (using steered MD/umbrella sampling) or introduce Gaussian potentials (in metadynamics). This either applies an external force on the phosphate ion or makes its energy well shallower, helping the collective variable (for instance, phosphate-Mg^{2+} distance) exit its initial energy minimum and explore other states.

the conformational sampling. Then, we present recent CG and multiscale models of MT dynamic instability. Finally, we highlight developments in models connecting cytoskeletal dynamics to the extracellular matrix through adhesion complexes (Chan and Odde 2008; Isomursu et al. 2022; Sens 2020; Bangasser et al. 2017; Elosegui-Artola et al. 2014; Andreu et al. 2021). Across these sections, we emphasize the biological insights that emerge. While covering the entirety of the literature on cytoskeleton modeling and simulations is unfeasible, we hope to provide an integrated perspective on the current trajectory of the field and highlight promising future directions for modeling approaches and integration across spatiotemporal scales.

2 | All-Atom MD Simulations of Cytoskeletal Filaments

Over the past decade, AA MD simulations have become indispensable for probing cytoskeletal filament dynamics, protein–protein interactions, and the molecular consequences of mutations (Chu and Voth 2005; Wells and Aksimentiev 2010; Plattner et al. 2017; Gill and McCully 2019). Advances in GPU-accelerated MD engines (Kutzner et al. 2015; Kondratyuk et al. 2021; Chen and Yang 2025), improved biomolecular force fields (Huang, Rauscher, et al. 2017), high-resolution cryo-EM structures, and enhanced sampling strategies (Ghanta et al. 2025; Wang et al. 2024), including those integrating data-driven modeling or machine learning (ML) (Wu et al. 2025; Feng and Mitran 2018; Guo et al. 2024), now enable atomistic simulations to capture both atomistic fluctuations and the barrier-crossing rare events underlying cytoskeletal assembly, remodeling and mechanotransduction.

2.1 | All-Atom MD Simulation Methods

Equilibrium MD simulations capture atomic motions under constant thermodynamic conditions by sampling conformations around local minima of the effective energy landscape (Figure 2A). However, many cytoskeletal processes, including phosphate release, cytoskeletal filament remodeling, and polymerization, may require crossing energy barriers that are not thermally accessible on standard simulation timescales. Enhanced sampling methods address this limitation by modifying the effective free-energy landscape through biasing potentials, non-equilibrium forces, or data-driven approximations

19493592, 0, Downloaded from https://onlinelibrary.wiley.com/doi/10.1002/cm.70221, Wiley Online Library on [25/11/2026]. See the Terms and Conditions (https://onlinelibrary.wiley.com/terms-and-conditions) on Wiley Online Library for rules of use; OA articles are governed by the applicable Creative Commons License

along selected collective variables (CVs) (Figure 2B). Techniques such as steered MD simulations, umbrella sampling, metadynamics, and ML–accelerated approaches (Zhu, Trizio, et al. 2025; Bernardi et al. 2015) have enabled the characterization of rare events and free-energy barriers underlying cytoskeletal dynamics.

Steered MD (SMD) simulations involve applying an external force or moving harmonic restraint to selected atoms to drive the molecular system along a reaction coordinate (Figure 3A). This approach is used to sample force-induced conformational changes such as unfolding pathways, receptor-ligand dissociation, and other non-equilibrium mechanisms. The resulting molecular configurations are also commonly used as starting structures for umbrella sampling. In umbrella sampling, harmonic restraints are applied to these configurations, and they are simulated in parallel, allowing the systems to sample overlapping regions of conformational space. The resulting biased probability distributions are subsequently unbiased and combined using the Weighted Histogram Analysis Method

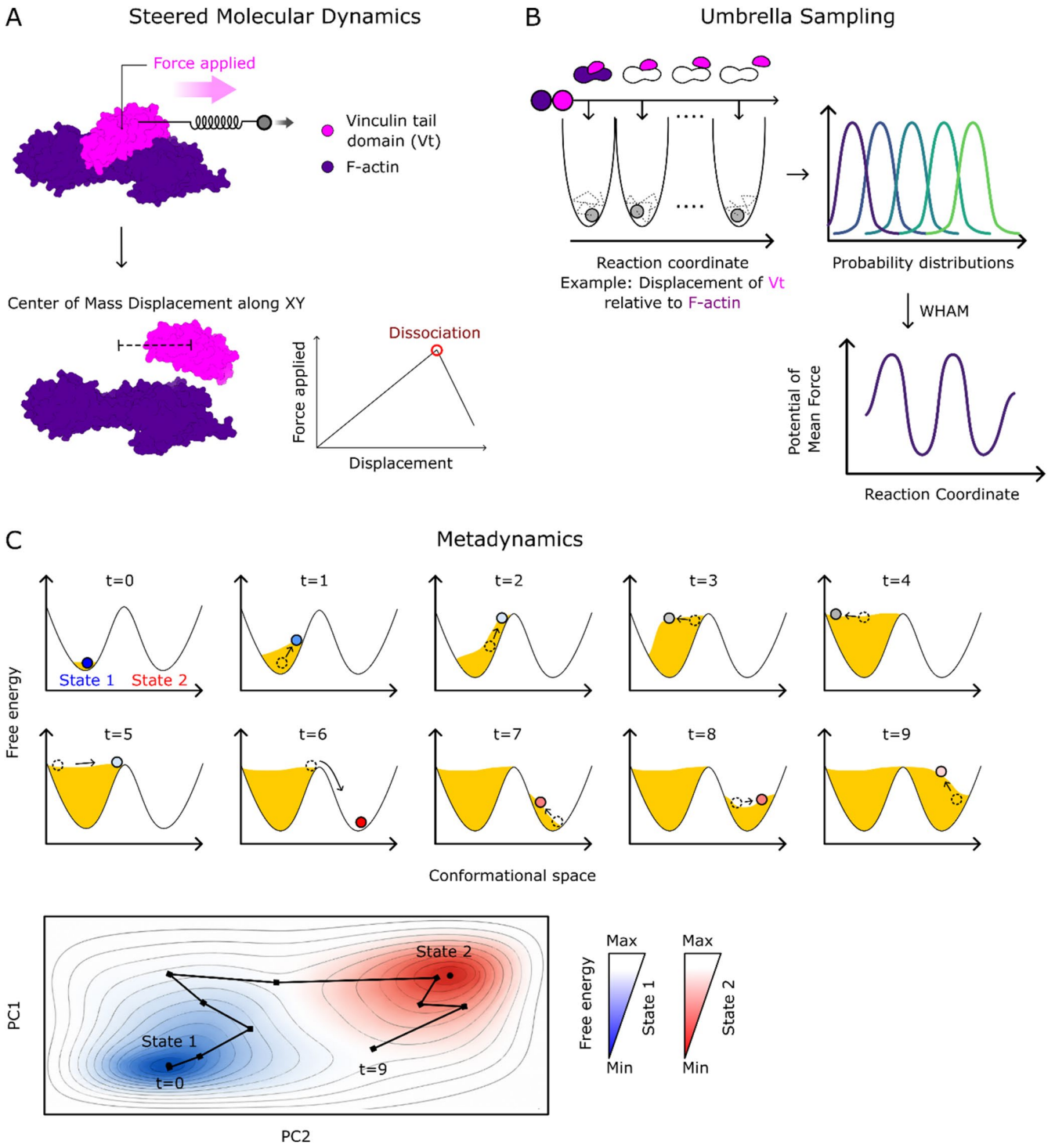

FIGURE 3 | Legend on next page.

19493592, 0, Downloaded from https://onlinelibrary.wiley.com/doi/10.1002/cm.70221, Wiley Online Library on [25/11/2026]. See the Terms and Conditions (https://onlinelibrary.wiley.com/terms-and-conditions) on Wiley Online Library for rules of use; OA articles are governed by the applicable Creative Commons License

FIGURE 3 | Common enhanced sampling techniques employed in studying cytoskeletal mechanics. (A) Steered molecular dynamics (SMD) simulations involve an applied force on a selected molecule (or molecular region) and pulling in a specified direction relative to another molecule (or molecular region). The pulled molecule is coupled to a virtual harmonic spring whose other end is linked to a dummy particle that constantly moves (constant velocity). If the pulled molecule continues to interact with the reference molecule during the pull, the virtual spring undergoes extension, and the pulling force continues to increase. In this example, the vinculin tail domain (Vt) is pulled relative to F-actin. Once Vt dissociates completely, the harmonic spring tension is released. (B) Following SMD, multiple structural snapshots can be extracted along the trajectory and used as starting configurations for umbrella-sampling. Each simulation samples a restrained region, or window, along the reaction coordinate, producing a biased probability distribution of conformations. In this example, the reaction coordinate is defined as the center-of-mass displacement of Vt relative to F-actin. Provided that sufficient overlap exists between probability distributions from neighboring windows, WHAM can combine these distributions to reconstruct the PMF. The resulting PMF reveals the relative free energies of the states and the free-energy barriers separating them. (C) In metadynamics simulations, Gaussian bias potentials are progressively deposited (shaded in yellow) into regions of the conformational space visited by the molecular system. In this example, we show a system initialized in state 1 at time (t) = 0. As the system explores different configurations, Gaussian bias potentials accumulate, filling up the free energy basin of state 1, gradually reducing the effective free energy barrier to transition to state 2. Once the system enters the free energy basin of state 2 at $t = 6$ and explores configurations around state 2, the Gaussian bias potentials can eventually facilitate its transition back to state 1. The 2D conformational space contour plot (defined by PC1 and PC2, for example) illustrates the explored states relative to the free energy minima of states 1 and 2, represented as blue and red regions, respectively.

(WHAM) to reconstruct a continuous potential of mean force (PMF). The PMF can then be used to determine relative free energies between conformational states (Torrie and Valleau 1977) (Figure 3B).

In metadynamics simulations, history-dependent Gaussian potentials are periodically deposited in CV space. The accumulated bias discourages repeated sampling of previously visited free-energy minima and promotes transitions into previously inaccessible regions of the free-energy landscape (Figure 3C). As sampling proceeds, the accumulated bias can be used to reconstruct the underlying free-energy surface (Laio and Parrinello 2002; Barducci et al. 2011).

These approaches are complementary and their use depends on the specific question and the system at play. SMD is particularly useful for generating mechanically driven pathways; umbrella sampling provides quantitative free-energy profiles along predefined coordinates; and metadynamics facilitates exploration of complex landscapes when transitions between states are difficult to sample directly. Their common purpose is to convert otherwise inaccessible molecular transitions into quantitatively interpretable mechanisms. These enhanced sampling methods have elucidated key cytoskeletal processes, including F-actin nucleotide hydrolysis (Beckett and Voth 2023), polymerization (Demosthene et al. 2023), Arp2/3-mediated branching (Singh et al. 2023; Laporte and Magistrato 2021), phosphate release (Wang et al. 2024; Oosterheert et al. 2023), twisting and flattening of G-actin subunits (Sridharan Iyer, Herman, et al. 2025), MT tip flaring (Wu et al. 2025; Igaev and Grubmuller 2022), and exposure of "cracked" F-actin sites under mechanical strain (Zsolnay et al. 2024).

ML-based enhanced sampling provides complementary strategies for overcoming limitations associated with manual CV selection and predefined biasing potentials. These approaches include data-driven identification of non-linear collective variables, adaptive optimization of biasing potentials, reinforcement-learning-guided exploration, and generative models that propose configurations or transition pathways. By learning molecular motions and iteratively directing simulations toward rare or insufficiently sampled regions, ML-based approaches can facilitate access to regions of conformational space that would otherwise be sampled only on much longer timescales in unbiased simulations (Zhu, Trizio, et al. 2025; Bernardi et al. 2015; Sidky et al. 2020; Mehdi et al. 2024).

Data-driven, equation-free approaches can further extend the effective timescales accessible to AA MD simulations by projecting dynamics onto a reduced set of structural variables, advancing these variables through coarse projective steps, and reconstructing corresponding atomistic snapshots for subsequent AA MD (Wu et al. 2025). Another ML emerging strategy is the Hybridizing Ions Treatment (HIT) model, which implements a hybrid solvent model where ions that are bound to protein complexes are treated as explicit atoms, whereas unbound ions are modeled implicitly (Sun et al. 2021, 2023).

Discrete molecular dynamics (DMD), in contrast, is an event-driven approach in which particles evolve through discrete collision events governed by discontinuous potentials (Proctor and Dokholyan 2016). While conventional MD simulations rely on continuous empirical forcefields where the system state evolves over uniformly distributed timesteps, DMD simulations evolve asynchronously from collision to collision, drastically reducing the computational time required to sample an event. This approach has been utilized to study the directional force-dependent interactions between actin and vinculin, and was combined with umbrella sampling to systematically explore their interaction energies (Chirasani et al. 2023). However, from this study, we note that the limitations of DMD include the reliance on discontinuous step potentials, which sacrifice atomistic vibrational details and the need to apply higher forces than those physiologically recorded to observe dissociation events within feasible computational timescales.

2.2 | Applications of All-Atom Equilibrium and Enhanced MD Studies of Microtubules and F-Actin

MTs exhibit distinct conformational states depending on nucleotide occupancy. Cryo-EM reconstructions have shown that while both GTP- and GDP-bound tubulin dimers favor a curved

19493592, 0, Downloaded from https://onlinelibrary.wiley.com/doi/10.1002/cm.70221, Wiley Online Library on [25/11/2026]. See the Terms and Conditions (https://onlinelibrary.wiley.com/terms-and-conditions) on Wiley Online Library for rules of use; OA articles are governed by the applicable Creative Commons License

conformation in isolation, GTP-bound dimers are forced into a straight conformation within assembled MT lattices (Alushin et al. 2014; Zhang et al. 2015). GTP hydrolysis to GDP acts as an allosteric trigger that stores significant elastic strain within the lattice. This strain effectively weakens lateral and longitudinal subunit contacts, reducing lattice rigidity and leading GDP-bound regions of the lattice to depolymerize once the stabilizing GTP cap at the MT tip is lost (Zhang et al. 2015; Ti et al. 2018). Equilibrium AA MD simulations have modeled MT segments composed of 14 protofilaments (PFs) with up to 6 stacked dimers per PF, representing multi-million atom systems. When initialized from straight cylindrical MT geometries, these simulations show a spontaneous relaxation at the MT plus ends toward splayed, outward-curving PF morphologies, regardless of the nucleotide state. However, these simulations also reveal that GDP-bound tips exhibit far higher propensity for splaying, and enhanced lateral instability (Wu et al. 2025; Igaev and Grubmuller 2022; Tong and Voth 2020). While GTP- or GMPCPP-bound PFs retain higher bond stability that resists splaying, the GDP-bound PFs rapidly adopt their preferred bent conformations and peel radially outward.

Smaller-scale MT models have clarified mechanisms of post-translational modifications, electrostatic regulation of MT-associated protein binding (Castro et al. 2023; Guo et al. 2023), and the energetics of motor–MT interactions (Guo et al. 2024; Nasrin et al. 2024). MD simulations comparing native Tau to its modified counterparts show that lysine acetylations, remove positive charges and alter the protein's overall electrostatics, which directly hampers its association with the negatively charged tubulin subunit (Castro et al. 2023). Similarly, hyperphosphorylation adds negative charges that induce electrostatic repulsion from the tubulin wall and trigger a folded conformation, which prevents MT attachment.

In parallel, AA MD simulations of F-actin have resolved interactions with regulatory proteins and elucidated molecular determinants of filament organization. Studies of fascin-mediated bundling (Wu et al. 2024), tropomyosin binding (Lehman et al. 2018), Arp2/3 docking (Sridharan Iyer, Wu, et al. 2025), and actin nucleus stabilization (Robinson et al. 2025) reveal residue-level mechanisms governing filament assembly, branching, and mechanical reinforcement. Well-tempered metadynamics has clarified phosphate release from ADP–Pi F-actin, identifying Mg^{2+} dissociation as a rate-limiting step (Dama et al. 2014; Mukadum et al. 2024; Chou and Pollard 2019; Wriggers and Schulten 1999) (Figure 2B). Equilibrium and SMD simulations have also elucidated Arp2/3-mediated branching, revealing energy barriers between inactive and active conformations and demonstrating how N-WASp binding stabilizes branch-competent states (Singh et al. 2023; Laporte and Magistrato 2021).

To capture how chemical reactions occur inside biological structures, hybrid quantum mechanics/molecular mechanics (QM/MM) simulations can be performed (Suh et al. 2024). Standard MD simulations rely on classical force fields that approximate atoms as point masses and treat covalent bonds as fixed, unbreakable springs. Therefore, they are fundamentally incapable of simulating the breaking or forming of covalent bonds. The QM/MM approach overcomes this limitation by dividing the system into two zones: (i) the precise active site where the chemical reaction takes place is modeled using quantum mechanics (QM) to track electronic rearrangements, and (ii) the rest of the biochemical system is modeled using molecular mechanics (MM) to aid in speed-up of calculations. A computational study applied this approach to an all-atom MT lattice model and simulated the chemical hydrolysis event of tubulin dimer-bound GTP to GDP. The simulations revealed that GTP hydrolysis is regulated by the compaction of the interdimer complex, that is, a reduction in distances between longitudinally neighboring dimers from 42 to 40.5 Å in the MT lattice (Beckett and Voth 2023). In the compacted lattice, GTP hydrolysis is highly favored with an energy barrier of 24.0 ± 0.2 kcal/mol, where the α-tubulin residue α-E254 acts as the direct catalytic base to deprotonate the lytic water. In the expanded MT lattice, the energy barrier for hydrolysis of GTP is 6.3 ± 0.5 kcal/mol higher, as the increased interdimer distance breaks a critical inter-subunit salt bridge between α-R2 and β-E69, which leads to a less efficient reaction pathway. Although absolute reaction barriers may exceed experimental estimates due to density functional approximations, these comparative simulations demonstrate that lattice compaction is a prerequisite for GTP hydrolysis. Therefore, by adopting QM/MM simulations to study chemical reaction sites, an extra layer of atomistic detail underlying biochemical mechanisms on a larger scale can be uncovered.

2.3 | Force-Dependent Mechanochemical Behavior of F-Actin and Microtubules

Mechanical forces reconfigure cytoskeletal filaments and their binding partners. SMD studies have characterized an approximately 30 Å movement of Arp2 during activation, in which structural elements rotate around a pivot point within an alpha-helical region of ARPC4 to align Arp2 and Arp3 into a short-pitch helical arrangement (Dalhaimer and Pollard 2010). Further simulations suggest a multistep pathway in which interactions with the mother F-actin stabilize subunit flattening in Arp3, while WASP proteins and recruited actin monomers stimulate the short-pitch conformation (Singh et al. 2023; Ding et al. 2022). Additionally, SMD has revealed how the structural transitions of cardiac tropomyosin follow an azimuthal rotational path around the axis of the F-actin (Williams et al. 2018). Another study showed that tensile loading in F-actin can induce the emergence of metastable "cracked" states, in which one PF breaks before full filament severing, due to disruption of the critical D-loop to W-loop connection between longitudinal subunits. These cracks expose cryptic binding sites for mechanosensitive regulators such as LIM-domain proteins (Zsolnay et al. 2024). In addition to exposing cryptic sites, mechanical forces in the piconewton range can directly modulate the kinetics of F-actin interactions with binding proteins by forming "catch bonds," a phenomenon in which bond lifetime increases under mechanical load. Catch bonds are essential in mechanobiology, as they enable proteins such as vinculin to reinforce cellular adhesions by linking them to the actin cytoskeleton (Huang, Bax, et al. 2017). Metadynamics MD simulations showed that catch bonds form when directional pulling shifts vinculin between weakly and strongly bound states relative to F-actin, with both states exhibiting intrinsic catch-bonding behavior (Peña Ccoa et al. 2025). In summary, enhanced sampling MD simulations have served as a powerful

19493592, 0, Downloaded from https://onlinelibrary.wiley.com/doi/10.1002/cm.70221, Wiley Online Library on [25/11/2026]. See the Terms and Conditions (https://onlinelibrary.wiley.com/terms-and-conditions) on Wiley Online Library for rules of use; OA articles are governed by the applicable Creative Commons License

"computational microscope" to probe how force transmission is coupled to molecular-level conformational changes in protein–protein interactions associated with actin filaments.

In MTs, force-dependent AA MD simulations link MT-associated protein interactions to changes in lattice stability and mechanochemical response (Guo et al. 2024; Castro et al. 2023; Nasrin et al. 2024; Cannariato et al. 2024). MD simulations reveal that stretching tubulin heterodimers decreases their interaction energy with the dynein microtubule-binding domain, leading to faster detachment rates and more frequent stepping (Nasrin et al. 2024). Multiscale analysis combining MD with elastic network modeling has further shown that Taxol binding induces conformational changes in the M-loop region, thereby stabilizing lateral inter-PF interactions and increasing the overall deformability and flexibility of MTs (Cannariato et al. 2024). Furthermore, the affinity and mechanical response of MT-associated proteins (MAPs) like Tau are significantly modulated by post-translational modifications (PTMs) such as acetylation and phosphorylation (MacTaggart and Kashina 2021). These PTMs alter the electrostatic landscape and association of MAPs to MTs (Castro et al. 2023). To accurately capture these force-driven MT-protein interactions, the ML-based "Hybridizing Ions Treatment-2" (HIT-2) model was used to explicitly treat bound ions at highly charged kinesin-MT interfaces, as these ions significantly impact electrostatic binding forces (Guo et al. 2024). Specifically, the model found that interfacial sodium ions, mostly localized on β-tubulin, increase the surface area of oppositely charged interfaces. The key observation was that the electrostatic potential analyzed from simulations using the HIT-2 hybrid model indicated a greater attractive interface between the Ncd motor and the MT tubulin dimers than when using the implicit solvent model. Although the magnitudes of electrostatic binding forces calculated from simulations with the two models differed, the net forces between the Ncd motor and the MT tubulin dimer were attractive in nature. Together, these studies provide structural insights into how mechanical load regulates cytoskeletal structure and protein recruitment at the molecular levels.

3 | Coarse-Grained and Multi-Scale Models of Microtubules

CG approaches enable larger and/or longer simulations than AA MD by mapping groups of atoms to effective interaction sites. This smoothens the underlying energy landscape by eliminating high-frequency particle and bond fluctuations, allowing higher timestep integration. In comparison, AA MD simulations require a lower timestep (~2 fs) integration to simulate high-frequency bond (O—H, N—H, C—H) vibrations. For instance, intermediate-resolution frameworks like the Martini forcefield map ~4 heavy atoms (including associated hydrogens) to one bead. Although this has enabled simulations of larger systems (~hundreds of nanometers) for longer (typically up to ~tens of microseconds) compared to AA MD simulations, its resolution limits the study of larger molecular systems on the micrometer scale and/or mechanisms occurring on the timescales of milliseconds and above. To simulate processes on these spatial and temporal scales, ultra-coarse-grained (UCG) approaches are necessary to coarse-grain the systems to lower resolutions. CG models may be parameterized bottom-up from AA simulations via force matching, Boltzmann inversion, or relative entropy minimization (Shell 2008), implemented in tools like OpenMSCG (Peng et al. 2023), or using parameterized frameworks such as the Martini force field (Marrink et al. 2007; Souza et al. 2021).

3.1 | Martini-Based Coarse-Graining and Elastic Network Modeling

Martini-based CG utilizes a systematic building-block approach to represent small fragments of ~4 heavy atoms and their associated hydrogen atoms as specific bead types depending on their chemical properties (Marrink et al. 2023). The force field comprises bead types, masses, and charges, with non-bonded pairwise interactions governed by Lennard-Jones and Coulombic potentials, and local conformational flexibilities modeled by standard harmonic bonds and angles. Since isotropic beads cannot natively capture the directionality of hydrogen bonding, an elastic network model (ENM) is superimposed on this foundation to maintain structural stability. The ENM applies a network of harmonic springs to backbone bead pairs within a specified distance cutoff (~0.9 nm in Martini 3) based on an atomistic reference structure, which is usually an experimentally resolved or predicted model. This approach constrains proteins to their native folded states without the need for explicit hydrogen-bond modeling.

Martini-based CG modeling for MTs has incorporated heterogenous elastic network (hENM) model representations derived from AA MD fluctuations to accurately model MT dynamics (Sahoo and Hanson 2025). In the study of large-scale MT lattice models, standard uniform elastic networks often fail to preserve the structure of the lattice, leading to PF twisting or the rapid loss of inter-tubulin dimer contacts. To address this, the hENM model was based on an iteratively redefined distance-based elastic network (IDEN), which was developed by removing highly dynamic regions and scaling spring constants of elastic network bonds inversely proportional to the variance of AA backbone distances. This approach enabled the simulation of a ~200 nm MT lattice structure composed of ~6 million beads while accurately reproducing mechanical properties such as flexural rigidity (Sahoo and Hanson 2025). To construct this IDEN framework, the initial elastic network was sub-sampled by removing conformational outliers that exceeded three standard deviations of the AA reference fluctuations, filtering out highly dynamic regions. Iterative optimization of the remaining bonds reduced the total number of harmonic restraints by roughly 7.3%–7.8%, converging on average spring constants between 93.1 and 125.4 kJ/mol. This successfully relieved local structural tension while maintaining the lattice's stable cylindrical form. To prevent the artificial conformational compaction typical of standard Martini 3 in unstructured regions, protein–water interactions were scaled up by 6% to accurately match the end-to-end distances of the highly charged C-terminal tails (α-tail of 19 residues and β-tail of 18 residues). This explicit-solvent model revealed that acidic residues on the disordered α-tails form long-lived, stabilizing electrostatic interactions with basic residues in the folded β-tubulin of adjacent dimers, running in the minus direction along a PF. Furthermore, the model captured

19493592, 0, Downloaded from https://onlinelibrary.wiley.com/doi/10.1002/cm.70221, Wiley Online Library on [25/11/2026]. See the Terms and Conditions (https://onlinelibrary.wiley.com/terms-and-conditions) on Wiley Online Library for rules of use; OA articles are governed by the applicable Creative Commons License

a localized, 5-fold accumulation of monovalent ions at the MT surface. Mechanically, this parameterized lattice yielded an experimentally consistent flexural rigidity of 12.6–45 pN.mm^2 depending on the simulation boundary conditions, successfully reproducing both the progressive structural stiffening observed with sequential GMPCPP capping and the peeling dynamics of individual PFs at the MT plus end.

A limitation of the standard Martini 3 framework is the overestimation of protein–protein interactions, which often results in overly compact conformational ensembles for flexible proteins (Thomasen et al. 2024; Binder et al. 2025). This bias can be mitigated by rescaling non-bonded interactions, such as increasing protein-water interaction strength by ~10% to match experimental small-angle X-ray scattering (SAXS) data (Thomasen et al. 2024, 2023). In addition, to circumvent the lack of explicit parameters, that is, bead-type assignments, bonded topologies (bonds, angles, dihedrals), and non-bonded interaction potentials, for molecules such as GTP or GDP, nucleotide-dependent conformational states were encoded directly via elastic network constraints (Sahoo and Hanson 2025) in the MT model. Therefore, it must be noted that there are inherent shortcomings of the native forcefield and appropriate measures, such as scaling protein-water interactions or parametrization of small molecules (Szczuka et al. 2026), are required prior to simulating certain biological systems accurately. Given that Martini-based CG MD simulations are based on intermediate CG resolution modeling (between AA and other CG approaches), they can be used to study (sub-cellular) biomolecular systems spanning hundreds of nanometers and up to tens or hundreds of microseconds depending on the size of the system. This represents a considerable acceleration in sampling compared to AA MD. Nonetheless, the computational cost of modeling explicit solvent and residue-level degrees of freedom makes cellular-level system sizes (micrometer-scale) and timescales (micro- to milliseconds) inaccessible to Martini-based models. This continues to motivate the development of lower-resolution CG modeling, BD and multi-scale approaches with implicit solvent, and stochastic modeling to study large-scale cytoskeletal dynamics (Skora et al. 2025; Xue et al. 2026; Gudimchuk et al. 2020; Hemmat and Odde 2021; Alexandrova et al. 2022; Lyman et al. 2008; Zhu, Zhang, et al. 2025; Kalutskii et al. 2025).

3.2 | Coarse-Graining and Backmapping Tools

OpenMSCG implements bottom-up coarse-graining by mapping AA structures to CG representations with a user-defined number of beads per molecule. The choice of the number of beads per molecule can be optimized using the essential dynamics coarse-graining (EDCG) method to minimize the loss of structural covariance while retaining significant low-frequency motions in the CG model (Peng et al. 2023; Zhang et al. 2008). To derive the interaction potentials between these beads, OpenMSCG supports several workflows such as Boltzmann inversion (BI), force-matching (FM), relative entropy minimization (REM), and hENM construction (Peng et al. 2023): (i) BI directly calculates pairwise potentials by mathematically inverting probability distributions of feature variables, such as radial distribution functions, obtained from AA trajectories; (ii) FM optimizes tabulated potentials by minimizing the least-squared difference between the CG forces and the reference forces mapped from the AA trajectory; (iii) REM iteratively refines potential parameters with a goal that the CG model should sample the same conformational space as the reference AA model, and (iv) hENM parameterizes the force constants of pairwise harmonic springs within a distance cutoff to reproduce mean-squared distance fluctuations calculated from reference AA simulations. Furthermore, OpenMSCG can generate CG models from AA MD simulation data generated by widely used MD software, such as GROMACS (Van Der Spoel et al. 2005), LAMMPS (Thompson et al. 2022), and NAMD (Phillips et al. 2005), whereas CG parameters generated by OpenMSCG are tabulated numerical potentials that can be parsed by GROMACS and LAMMPS to perform CG simulations.

Regardless of the choice of CG resolution, CG simulations can be performed in conjunction with AA resolution simulations via a multi-scale approach. Backmapping is a method that enables such an approach by reconstructing AA coordinates from CG representations. Traditionally, a CG model is first simulated for the molecular system to reach equilibrium at the macro level, followed by backmapping, which reveals the AA coordinates and topology of the equilibrated system, enabling AA simulations to refine interactions in greater detail. For example, MSBack recovers AA coordinates by generating α-carbon trace distributions, followed by reconstruction of missing side chain and backbone atoms, and a final unrestrained energy minimization to resolve steric clashes (Waltmann et al. 2025). This process allows validation of CG structures (Lombardi et al. 2016), assessment of mutation effects on filament mechanics (Badaczewska-Dawid et al. 2020), and generation of starting structures for downstream AA MD or QM/MM simulations (Shmilovich et al. 2022). Compatible with the Martini framework, there are two backmapping tools that can be used to study cytoskeletal proteins in multi-scale resolution. The first is CG2AT2 (Vickery and Stansfeld 2021), which is a fragment-based backmapping algorithm that converts macromolecular complexes, including protein-membrane systems, from CG to AA resolution. It functions by rigidly aligning small AA fragments, which contain all necessary chemical and stereochemical information, to each CG bead. CG2AT2 uses mappings derived from a fragment database linked to commonly used AA forcefields such as CHARMM36m (Huang, Rauscher, et al. 2017), AMBER (Lindorff-Larsen et al. 2010), GROMOS (Oostenbrink et al. 2004), and OPLS (Kaminski et al. 2001) to reintroduce AA topology and stereochemistry to the backmapped model. Secondly, GLIMPS (Louison et al. 2021) is an ML-based CG to AA resolution transformation that uses a matched set of high- and low-resolution models while training. To use GLIMPS, an ensemble of existing AA structures of the target system must first be coarse-grained to generate a corresponding ensemble of CG structures using the Martinize tool (Kroon et al. 2025). Once GLIMPS is trained by the user on this matched set of AA and CG structures, a new CG structure can be used to reconstruct the corresponding AA coordinates. Unlike CG2AT2, GLIMPS does not require substructure templates, mappings, or forcefields for reference. Overall, these tools enable backmapping of CG models to AA resolution, using a range of techniques, thereby providing the scientific community with a foundation for employing multi-scale approaches.

19493592, 0, Downloaded from https://onlinelibrary.wiley.com/doi/10.1002/cm.70221, Wiley Online Library on [25/11/2026]. See the Terms and Conditions (https://onlinelibrary.wiley.com/terms-and-conditions) on Wiley Online Library for rules of use; OA articles are governed by the applicable Creative Commons License

3.3 | Brownian Dynamics, Thermokinetic Modeling and Ultra-Coarse-Graining

To address timescale limitations, multiscale strategies have combined AA MD, CG, BD, and thermokinetic modeling (Skora et al. 2025; Kalutskii et al. 2025). BD models neglect the inertial component of motion and integrate overdamped Langevin dynamics (Skora et al. 2025; Kalutskii et al. 2025). In one study, AA MD trajectories of short MT tips were coarse-grained to two beads per tubulin heterodimer (Skora et al. 2025), and interaction potentials between beads were derived via iterative Boltzmann inversion (IBI). The resulting force field contained harmonic longitudinal intra- and inter-dimer interactions and breakable Morse-type lateral α–α and β–β interactions. Hydrodynamic radii of α- and β-tubulin were estimated using the generalized Rotne–Prager–Yamakawa bead formalism (Zuk et al. 2018). Simulating this model over tens of microseconds reproduced spontaneous PF clustering, outward flaring, partial out-of-plane bending, and a progressive increase in PF curvature. Importantly, similar relaxation was observed for GTP- and GDP-bound tips, and the approximately linear dependence of PF curvature on distance from the MT tip agreed with cryo-electron tomography (cryo-ET) observations of curved PFs at growing MT tips (McIntosh et al. 2018).

Another CG strategy was developed which represented each tubulin dimer by three CG beads connected via stretchable and rotatable elastic interactions (Kalutskii et al. 2025). The bead placement was chosen to capture the intra- and inter-dimer hinge regions that facilitate PF bending and twisting. The mechanical parameters, including stretching, bending, twisting, and bending–torsional coupling, were derived from AA MD simulations. Unlike a purely elastic network, breakable longitudinal and lateral interactions were introduced so that PF–PF contacts could reorganize and individual tubulins or oligomers could dissociate. This model extended simulations of MT tips into the sub-millisecond-to-millisecond regime and revealed a dynamic competition between the tendency of individual PFs to curve and their tendency to form partially straightened clusters. GTP-bound MT tips formed larger and longer-lived PF clusters than GDP-bound ends, but these clusters also accumulated greater internal mechanical frustration and tensile strain, promoting PF rupture and producing relatively shorter and more uniform PF lengths. In contrast, GDP-bound ends more frequently became trapped in configurations containing long, uneven PFs or PF pairs, less favorable to adopt a straight cylindrical lattice and were therefore prone to shortening (Kalutskii et al. 2025).

Multiscale modeling can also transfer AA-derived energetics directly into kinetic parameters of MT assembly. A study calculated tubulin–tubulin interaction free-energy landscapes using AA MD combined with umbrella sampling, and subsequently incorporated the potentials of mean force into BD simulations of tubulin association with and dissociation from PF tips (Hemmat and Odde 2021). The BD calculations converted AA MD-derived interaction potentials into estimates of association and dissociation kinetics, as well as standard binding free energies. Their calculations indicated that the GTP-state longitudinal interaction is stronger than the GDP-state by approximately 4 kBT, whereas the lateral interaction was approximately nucleotide-independent. These parameters were then translated into thermokinetic and mechanochemical models operating over substantially longer timescales. Importantly, weakening of the longitudinal interaction alone could reproduce aspects of dynamic instability but produced unrealistically blunt MT tips. Introducing an additional nucleotide-dependent outward-bending preference of approximately 1.5 kBT following GTP hydrolysis enabled the model to recover more realistic tapered, splayed, and curling PF morphologies together with experimentally compatible assembly dynamics. This study therefore provides an example of information transfer from AA free-energy calculations, through BD-derived kinetic rates, to mesoscale predictions of MT growth, shortening, tip morphology, and catastrophe (Hemmat and Odde 2021).

Ultra-CG models omit biochemical detail to potentially explore macro-scale cytoskeletal behavior. For instance, a helix-based ultra-coarse-grained (HB-UCG) model (Zhu, Zhang, et al. 2025) represented each tubulin monomer in an MT lattice by one internal and one external bead yielding 4 UCG beads per tubulin dimer. Interactions between these sites were described using a Multiscale Virtual Particle Anisotropic Network Model (MVP-ANM), producing a compact harmonic-network representation that preserves the helical architecture and large-scale mechanical properties of the MT while greatly reducing the number of degrees of freedom. Since the helical representation in this framework could be extended without repeatedly coarse-graining increasingly large atomic structures, MTs as long as 35 μm were constructed and simulated. The model reproduced experimentally consistent relationships between MT contour length and persistence length and enabled CG simulations approaching the millisecond regime. In torsional simulations, one end of the MT was constrained while rotational displacement was applied to the opposite end. As a result, a 10-μm MT developed successive twists on the hundreds-of-microseconds timescale, permitting the propagation of torsional deformation and associated shear strain through the lattice to be quantified. Simulations of MT helicity further suggested that interactions between neighboring MTs may contribute substantially to the helicity measured experimentally in MT bundles (Zhu, Zhang, et al. 2025). Such ultra-coarse-graining is therefore particularly useful for interrogating persistence length, bending, twisting, shear, etc., at micrometer length scales that are inaccessible to AA MD or Martini-based CG MD simulations. However, this HB-UCG formulation intentionally omits much of the state-dependent intermolecular chemistry required to describe nucleotide hydrolysis, tubulin association and dissociation, or drug-binding energetics. Addressing these processes would require enrichment with state-dependent or breakable interaction potentials or coupling to MD simulations to obtain relevant molecular energetics data.

3.4 | Kinetic Monte Carlo Simulations and Hybrid Approaches

Kinetic Monte Carlo (kMC) frameworks provide a computationally efficient description of stochastic molecular events that govern MT dynamic instability. Hybrid BD–kMC models couple continuous filament mechanics to discrete biochemical transitions, capturing MT growth, shortening, and force-dependent behavior (Gudimchuk et al. 2020), while some models follow a kMC framework without BD implementation (Margolin

19493592, 0, Downloaded from https://onlinelibrary.wiley.com/doi/10.1002/cm.70221, Wiley Online Library on [25/11/2026]. See the Terms and Conditions (https://onlinelibrary.wiley.com/terms-and-conditions) on Wiley Online Library for rules of use; OA articles are governed by the applicable Creative Commons License

et al. 2012; Gardner et al. 2011). Standard kMC models, while sacrificing molecular detail, efficiently simulate rare catastrophe events over experimentally relevant timescales. In one of the studies with BD simulations (Gudimchuk et al. 2020), the simulation implementation is intertwined between (i) a "fast" BD layer that solves Langevin equations for tubulin dimers in the 13-PF MT lattice model, and (ii) a "slow" kMC layer that propels the simulation system in large (13 ms) time-steps and governs stochastic addition of tubulin and GTP hydrolysis. In these models, hydrolysis-induced weakening of inter-dimer bonds triggers PF breakage when the local potential energy exceeds an activation threshold. Additionally, hydrolysis increases PF bending stiffness, accumulating elastic strain in the lattice until the outward force exerted by the bent PFs ruptures lateral bonds. This framework also simulated MT growth and shortening under force via 13 beads representing the Dam1 ring complex, which couples MT dynamics to kinetochore function, demonstrating how MT lattice strain and tip curvature drive chromosome movement during mitosis. A subsequent study developed a four-state kMC model (Alexandrova et al. 2022), in which all events (association, dissociation, bending, and straightening of tubulin heterodimers) were governed solely by kinetic rates. Therefore, in contrast to AA MD (1–2 fs time-steps), CG MD (10–20 fs time-steps), and CG BD (~10–100 fs time-steps), standard kMC simulations proceed by selecting the next stochastic event. KMC models are computationally inexpensive and can simulate rare catastrophe events occurring on experimentally observed timescales (minutes). However, they need kinetic rates as input and these parameters are often derived phenomenologically rather than from first principle. Across formulations, these models consistently show that hydrolysis-dependent weakening of inter-dimer interactions governs PF curvature transitions and catastrophe initiation.

4 | The Role of Modern Structural Biology Experiments and Computing Methods in Studying Cytoskeletal Mechanics

Cryo-EM provides high-resolution structural information by analyzing purified components ex situ, a process that requires isolating them from their native environment. An example of its capability in studying cytoskeletal biology is the 3.9 Å cryo-EM structure of the Arp2/3 complex bound to a branched F-actin junction. In combination with biochemical assays, live-cell imaging, and MD simulations, this study revealed insights into the detailed interaction of the Arp2/3 complex with actin and its role in regulating branched actin assemblies (Ding et al. 2022). Building upon isolated structural snapshots, cryo-ET has revolutionized the study of cytoskeletal filaments by enabling visualization of their organization in their native cellular environment (Chakraborty et al. 2020). This method has aided in the structural elucidation of MT lattice defects, MT tip configuration, and PF clusters in mammalian cells (Kalutskii et al. 2025; Chakraborty et al. 2020; Atherton et al. 2018), the architecture of mammalian sperm axonemes (Chen, Greenan, et al. 2023), and identified unique structural features, such as F-actin segments residing within the MT lumen (Ventura Santos et al. 2023; Paul et al. 2020; Tsuji et al. 2024) and doublet MT (DMT) architectures along with DMT-associated proteins in mouse sperm cells (Tai et al. 2023). Moreover, a recent high-resolution cryo-EM study has shed light on DMT protein structure and mechanisms governing sperm function (Liu et al. 2026). Furthermore, the integration of optogenetics with cryo-ET has revealed the ultrastructure of mini filopodia precursors that drive membrane protrusion during lamellipodia extension (Inaba et al. 2025). These cryo-EM/ET-based experimental studies have made substantial contributions to the study of a variety of cytoskeletal structures and architectures. However, combining computational multiscale (AA, CG, and meso-scale) modeling can help use these static structural snapshots to reveal dynamic insights into their molecular mechanisms. For example, TIRF microscopy data on tubulin turnover combined with cryo-EM data and kMC modeling has demonstrated that elastic stress at lattice dislocations is sufficient to induce spontaneous MT self-renewal (Schaedel et al. 2019). Similarly, hybrid workflows can leverage cryo-EM-resolved structures and employ AA MD simulations to refine cytoskeletal structures at the atomic level and obtain data on their dynamic behavior in a more native context.

MT-associated proteins (MAPs) and actin-binding proteins (ABPs) play key roles in regulating cytoskeletal architecture and mechanics by aiding in filament cross-linking, bundling, and stabilization (Spiliotis and Nakos 2021; Cabrales Fontela et al. 2017; Bareja et al. 2025). However, a large number of full-length structures of these associated proteins remain unresolved by experimental approaches. AI-based structure prediction methods such as AlphaFold (Jumper et al. 2021; Abramson et al. 2024) and RoseTTAFold (Baek et al. 2021), can provide useful structural hypotheses, but intrinsically disordered regions remain difficult to predict because they occupy broad conformational ensembles (Holehouse and Kragelund 2024). Moreover, a study that combined cryo-ET and AlphaFold2-based structures of axonemal MTs and MAPs reported limitations, including (i) MAPs adopting different conformations in native environments, which are not accounted for by AlphaFold models, (ii) inability to resolve side chain densities by cryo-ET, which are key in defining protein–protein interfaces (Chen, Shiozaki, et al. 2023). To overcome these limitations, modeling techniques combined with simulations utilizing MD forcefields (Huang, Rauscher, et al. 2017; Thomasen et al. 2024; Lindorff-Larsen et al. 2010; Wang et al. 2025; Souza et al. 2025) in both AA and CG resolutions are key to filling the void and accurately modeling the biochemical structure and dynamics of these regions. CG approaches can accelerate conformational sampling over microsecond to millisecond timescales required to capture the diverse and native shapes of MAPs. Following a multi-scale approach, representative protein conformations from these CG trajectories can be backmapped to AA resolution structures. Subsequent AA MD simulations can be deployed to relax and fit these structures to cryo-EM/ET density maps, resolving thermodynamically optimal orientations of side chains in atomic resolution. Computational simulations can thus complement experimental observations and AI-based structure prediction, providing a holistic view of simulated cytoskeletal structures.

Quantum computing offers a fundamentally new paradigm for accelerating QM/MM simulations and navigating complex biomolecular energy landscapes more efficiently than classical algorithms (Nassir et al. 2025; Selvaraj et al. 2026). In a molecular context, the principle of "quantum superposition" allows a quantum computer to represent combinations of many possible states

19493592, 0, Downloaded from https://onlinelibrary.wiley.com/doi/10.1002/cm.70221, Wiley Online Library on [25/11/2026]. See the Terms and Conditions (https://onlinelibrary.wiley.com/terms-and-conditions) on Wiley Online Library for rules of use; OA articles are governed by the applicable Creative Commons License

of a molecular system simultaneously, while "quantum entanglement" captures strong correlations between different parts or degrees of freedom of the system that cannot be described independently. Quantum-assisted optimization methods may also exploit "quantum tunneling" -like behavior, allowing the search to pass through energy barriers rather than only climbing over them, which may facilitate escape from local energy minima more efficiently and frequently. Although these approaches remain in the early stages of biomolecular simulation, continued advances could eventually extend the spatial and temporal scales accessible to fine-grained modeling, potentially enabling studies of large, highly dynamic systems such as MTs undergoing dynamic instability. Presently, quantum computing faces limitations, including high hardware error rates, qubit decoherence, and noise that can distort energy measurements (Nassir et al. 2025; Selvaraj et al. 2026; Doga et al. 2024). Furthermore, resources for quantum computing remain inaccessible to a wide population of researchers, as there are only a limited number of such advanced machines globally.

5 | Mesoscale Models of Cytoskeleton and Adhesions

Mesoscale models represent a different level of coarse-graining from the CG models discussed above. Rather than retaining detailed representations, mesoscale approaches typically represent entire proteins or molecular complexes as mechanical elements (Bidone and Odde 2023; Bidone et al. 2014, 2017; Chen et al. 2021; Kim 2015; Kim, Hwang, and Kamm 2009; Kim, Hwang, Lee, and Kamm 2009; Borau et al. 2012). This reduction sacrifices molecular structural detail in exchange for access to collective behavior, over micron-scale dimensions and seconds-to-minutes timescales. At this scale, the scientific question also changes. AA and CG simulations primarily ask how molecular interactions determine protein structural dynamics and how state transitions occur within individual proteins, whereas mesoscale models ask how thousands of such interactions collectively generate higher-order assemblies of proteins, leading to diverse cytoskeletal architectures, force transmission pathways, and cellular behaviors. Mesoscale modeling of the cytoskeleton has developed along two complementary directions: modeling the self-organization of F-actin and MT networks, and modeling how those networks transmit force to the extracellular matrix (ECM). Simulation platforms such as Cytosim and MEDYAN provide frameworks for the first problem, while the motor-clutch framework and its extensions address the second (Chan and Odde 2008; Isomursu et al. 2022; Sens 2020; Bangasser et al. 2017; Elosegui-Artola et al. 2014; Andreu et al. 2021).

5.1 | Simulation Framework for Cytoskeletal Networks

Cytosim has been used in numerous studies of F-actin and MT network self-organization, ranging from actomyosin network morphology to spindle assembly and nuclear positioning (Nedelec and Foethke 2007; Loughlin et al. 2010; Nedelec 2002; Gibeaux et al. 2017; De Simone et al. 2016; Descovich et al. 2018; Cortes et al. 2020; Burdyniuk et al. 2018). Mechanically, filaments are modeled as discrete chains of connected points or segments (Chandrasekaran et al. 2019). To maintain a constant filament contour length while allowing the filaments to bend, buckle, or fluctuate, Cytosim utilizes an implicit integration method with algebraic constraints, which allows for the use of relatively large timesteps of 2–5 ms (Nedelec and Foethke 2007; Chandrasekaran et al. 2024). Filaments can explicitly interact with motors, crosslinkers, or nucleators, with binding and unbinding kinetics implemented as stochastic transitions governed by rate constants. The framework was originally validated by reproducing analytical and experimental benchmarks, including the buckling and relaxation dynamics of semiflexible fibers, the thermal fluctuation spectrum of filaments, and the self-organization of motor-driven asters (Nedelec and Foethke 2007). Recent applications have studied how protein kinetics shape network architecture. In simulations exploring the formation of an F-actin kinetic trap within liquid-like VASP/Arp2/3 protein droplets, VASP tetramers were modeled as spherical crosslinkers (radius = 30 nm) with four binding sites and a 30 nm binding-search radius. Actin elongation rates were set to 10.3 nm/s across elongation timescales of 10–600 s (Chandrasekaran et al. 2024). By parametrically varying binding and unbinding rates from 1×10^{-4} to $10\,s^{-1}$, with unbinding following force-dependent slip-bond kinetics per Bell's law (Chandrasekaran et al. 2024; Winkelman et al. 2014), the study revealed that shell, ring, or disk architectures arise from the relative kinetics of VASP-actin interactions. Notably, rings only form within an intermediate window of unbinding rates that is fast enough to permit reorganization but slow enough to sustain bundling. Using graph-theoretic analysis, studies have addressed how multivalent actin-binding proteins reshape actomyosin network morphology (Winkelman et al. 2014). They demonstrated that network connectivity and mechanical percolation can be predicted directly from the valency and binding kinetics of crosslinking proteins.

For MT simulations, Cytosim explicitly represents MTs with dynamic instability, alternating between growth and shrinkage phases separated by stochastic catastrophe and rescue transitions. Early simulations challenged the basic assumption that motor proteins are sufficient on their own to contract microtubule networks. Cytosim demonstrated that adding motors alone merely causes MTs to slide past each other without generating network contraction. More recent studies have examined what happens when highly processive molecular motors undergo liquid–liquid phase separation into dense clusters and evaluated the interplay between plus end versus minus end motors for spindle self-organization.

MEDYAN (Mechanochemical Dynamics of Active Networks) extends this class of models by explicitly coupling stochastic reaction–diffusion chemistry to filament mechanics, allowing polymerization, crosslinker binding, and motor activity to feedback on network-scale force generation (Popov et al. 2016). MEDYAN represents each semi-flexible filament as a series of connected cylindrical segments; crosslinkers, myosin motors, and branching/nucleating proteins (e.g., Arp2/3-mediated branching, formin-mediated nucleation) are represented as auxiliary mechanical elements attached to these cylinders. The core innovation relative to Cytosim is a four-step "mechanochemical loop": (1) a spatially resolved Gillespie stochastic simulation algorithm (SSA) evolves the chemical state of the network

19493592, 0, Downloaded from https://onlinelibrary.wiley.com/doi/10.1002/cm.70221, Wiley Online Library on [25/11/2026]. See the Terms and Conditions (https://onlinelibrary.wiley.com/terms-and-conditions) on Wiley Online Library for rules of use; OA articles are governed by the applicable Creative Commons License

(polymerization, depolymerization, binding/unbinding, motor stepping, diffusion of unbound species) over a chemical time-step; (2) these chemical events locally deform the network by adding or removing elements; (3) the resulting configuration is relaxed to a new force balance using conjugate-gradient energy minimization; and (4) the newly equilibrated mechanical stresses feed back to update chemical rate constants (e.g., via slip-bond, catch-bond, or biphasic force-dependent kinetics), closing the loop. This iterative alternation between explicit 3D reaction–diffusion chemistry and mechanical equilibration is the key distinction from Cytosim, which integrates mechanics and binding/unbinding kinetics simultaneously within a single continuous Langevin framework rather than resolving reaction–diffusion transport of diffusing chemical species explicitly.

MEDYAN has been adopted broadly to dissect how tensile loading drives cytoskeletal remodeling ahead of downstream biochemical signaling (Li et al. 2020). Simulations of actin networks subjected to stepwise AFM-like tensile pulls revealed that mechanical alignment and bundling of filaments along the force axis occurs within seconds, far faster than the minutes-scale biochemical remodeling (crosslinker reorganization, myosin recruitment) that follows, supporting a "mechanics-before-chemistry" model of force-induced cytoskeletal adaptation that had not been directly demonstrated computationally before. MEDYAN has also been used to understand how myosin and α-actinin jointly tune stress-fiber contractility under tension (Ni et al. 2023), showing that contractile force output is a non-monotonic function of α-actinin crosslinker density, with an optimal crosslinker concentration maximizing force transmission to focal adhesions. Contractile force also depends on the relative rates of myosin motor engagement versus crosslinker-mediated network integration, providing a mechanistic, quantitative understanding of stress-fiber force. Other applications of MEDYAN include probing actin bundle polarity sorting, ring contractility, and avalanche-like force propagation in branched networks (Chandrasekaran et al. 2019; Ni et al. 2022; Liman et al. 2020): these studies showed that myosin-driven polarity sorting alone (independent of filament buckling asymmetries) is sufficient to drive network contraction, that crosslinker concentration thresholds govern the transition from disordered actomyosin meshwork to bundled, contractile ring-like structures relevant to cytokinesis, and that mechanical stress propagates through branched actin architectures via discrete, avalanche-like rearrangement events whose size distribution can be predicted using network-science and machine-learning approaches applied to the underlying MEDYAN-simulated connectivity, a previously unrecognized statistical signature of force propagation in branched cytoskeletal networks.

5.2 | The Motor-Clutch Framework

Understanding how cytoskeletal networks interact with their environment requires shifting focus from filament rearrangements to force transmission at the cell-substrate interface. The motor–clutch framework is widely used to model how cells sense and respond to substrate stiffness. As we scale up to the cellular level, modeling evolves from structural dynamics representation of proteins and networks into functional frameworks of force transmission and ECM coupling. In the motor–clutch model, the whole F-actin network is represented as a rigid rod, and adhesions are represented as point particles ("clutches") that create intermittent connections between F-actin and the substrate. Each clutch, modeled as an elastic spring of stiffness k_c (5 pN/nm) (Chan and Odde 2008; Fisher et al. 1999), binds the substrate with a constant on-rate k_{on} and unbinds with an off-rate k_{off} (Figure 4A). Actin motion is driven by implicit motors pulling F-actin backward at velocity $v_{filament}$. The stochastic engagement of adhesion "clutches" resists F-actin flow and transmits force to the substrate (Chan and Odde 2008; Isomursu et al. 2022; Bangasser et al. 2017; Elosegui-Artola et al. 2014; Venturini and Saez 2023) (Figure 4A). When bound, the clutch force is: $F_C = k_c\left(x_i - x_{sub}\right)$, where x_i is the clutch position, and x_{sub} is the substrate position. In the initial formulation (Chan and Odde 2008), k_{off} was force-dependent and followed slip-bond kinetics per Bell's law (Bell 1978): $k_{off}(F) = k_{off}^0 exp\left(\frac{F_c}{F_b}\right)$, where k_{off}^0 is the unloaded off-rate, F_c is the clutch force and F_b is the rupture force, (~2–5 pN for integrin–talin–actin linkages (Chang et al. 2016; Hirata et al. 2014; Nordenfelt et al. 2016)). Subsequent extensions of the motor-clutch framework have used constant off-rates or incorporated catch-slip (biphasic) kinetics to incorporate more complex, force-strengthened unbinding clutch behavior (Bangasser et al. 2013; Kong et al. 2009; Elosegui-Artola et al. 2018). As multiple clutches share load, retrograde flow slows according to: $v_{filament} = v_u\left(1 - \frac{k_{sub} * x_{sub}}{F_{stall}}\right)$, where v_u is the unloaded myosin velocity, k_{sub} is the substrate stiffness (~0.01–100 kPa and F_{stall} is the total myosin stall force, given as: $F_{stall} = n_m * F_m$). Here, F_m is the force required to stall one myosin motor (~2 pN) and n_m is the number of motors (Molloy et al. 1995). On soft substrates, clutches detach before substantial force accumulates, while on stiff substrates rapid force loading leads to premature rupture. Maximal traction occurs at intermediate stiffness, where multiple clutches share load prior to failure (Chan and Odde 2008).

5.3 | Recent Advances in the Motor-Clutch Framework

To capture substrate rigidity sensing across diverse cell types and more complex mechanical environments, recent frameworks have expanded the classic motor–clutch model beyond uniform, memoryless springs. By treating mechanosensing as inherently history-dependent (past force affects future behavior) and spatially heterogeneous (adhesions aren't identical everywhere), these advances incorporate multiple adhesion proteins, force-dependent protein unfolding, and viscoelastic substrates (Venturini and Saez 2023; Campbell et al. 2023; Grudtsyna et al. 2023; Honasoge et al. 2023; Elosegui-Artola et al. 2016; Pulido Cifuentes et al. 2024; Alonso-Matilla et al. 2023; Gong et al. 2018; Liu et al. 2025). Mechanistically, force-dependent talin unfolding recruits vinculin to stabilize load-bearing connections, while catch-bond behavior enhances clutch lifetime under moderate force. Computational studies reveal that these mechanisms create non-linear feedback between filament flow, adhesion lifetime, and substrate stiffness, offering a mechanistic explanation for rigidity sensing and durotaxis (Grudtsyna et al. 2023; Honasoge et al. 2023; Lin and Forscher 1995; Suter and Forscher 2001; Owen et al. 2022). Simultaneously, coupling clutch engagement with actin polymerization, including

19493592, 0, Downloaded from https://onlinelibrary.wiley.com/doi/10.1002/cm.70221, Wiley Online Library on [25/11/2026]. See the Terms and Conditions (https://onlinelibrary.wiley.com/terms-and-conditions) on Wiley Online Library for rules of use; OA articles are governed by the applicable Creative Commons License

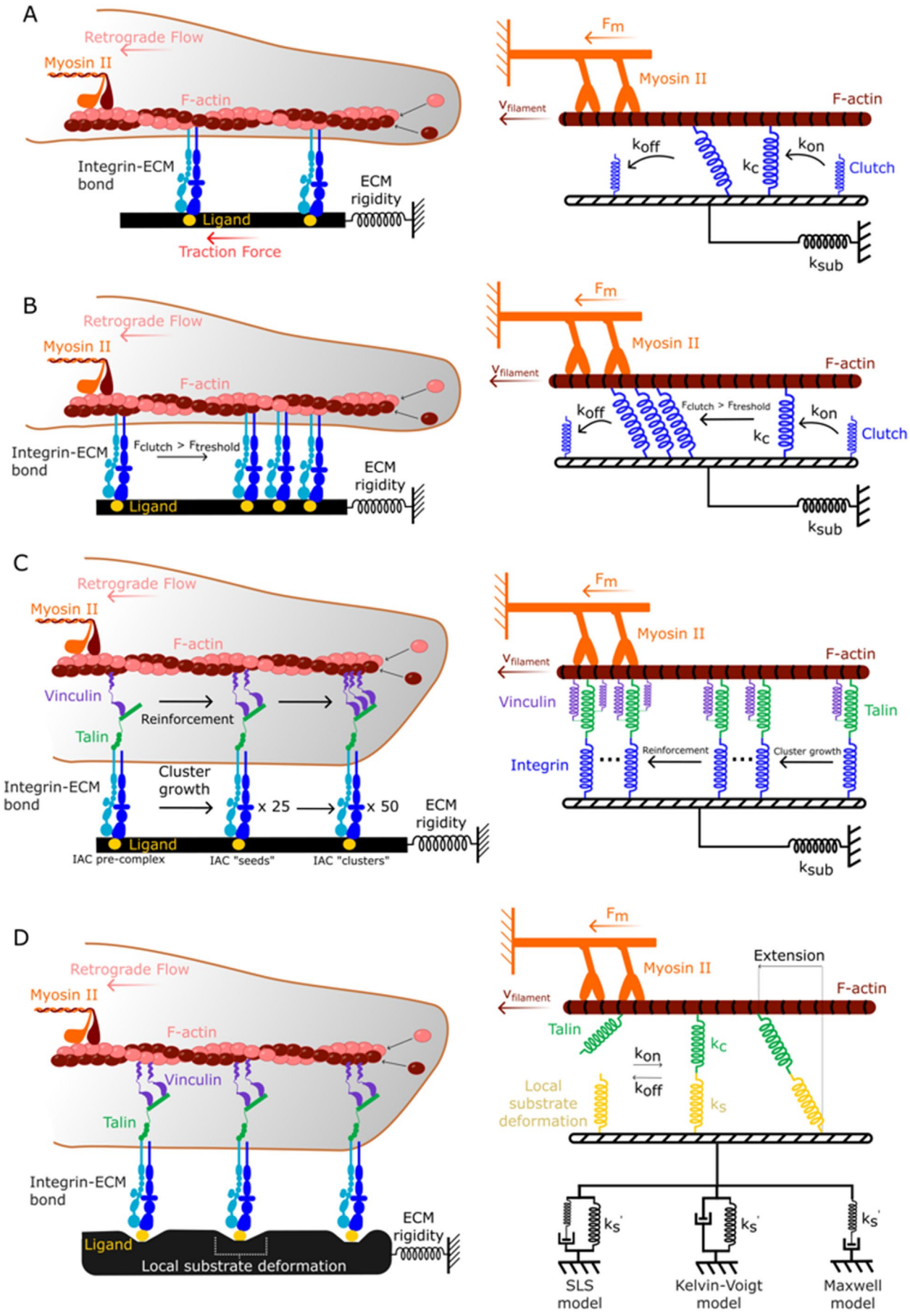

FIGURE 4 | Legend on next page.

19493592, 0, Downloaded from https://onlinelibrary.wiley.com/doi/10.1002/cm.70221, Wiley Online Library on [25/11/2026]. See the Terms and Conditions (https://onlinelibrary.wiley.com/terms-and-conditions) on Wiley Online Library for rules of use; OA articles are governed by the applicable Creative Commons License

FIGURE 4 | Evolution of molecular clutch models. In each panel, the left side illustrates the biological adhesion process, while the right side presents the corresponding mechanical representation. (A) Early molecular clutch model. Integrin–ECM bonds are elastic clutches that stochastically engage and disengage under actin retrograde flow. Clutch behavior is governed by force-dependent unbinding, clutch stiffness k_c, and the balance between actin velocity and transmitted load (Chan and Odde 2008). (B) Force-threshold reinforcement model. Clutches that bear forces above a threshold increase their stability. The mechanical representation incorporates this via force-sensitive unbinding rates $k_{off}(F)$, and reinforcement rules triggered when $F_{clutch} > F_{threshold}$ (Pulido Cifuentes et al. 2024). (C) Seed and cluster models incorporating talin and vinculin mechanics. Integrin adhesion complex "seeds" recruit additional clutches to form growing clusters. These formulations explicitly represent talin extension, vinculin recruitment, and mechanical reinforcement based on talin unfolding. The mechanical diagrams include multi-element intracellular springs, changes in k_c during talin extension, and cooperative binding dynamics that promote cluster growth (Honasoge et al. 2023). (D) Models incorporating local substrate deformation and viscoelastic ECM. Local substrate deformation at the adhesion site is distinct from global substrate stiffness, allowing the model to capture how traction forces deform the ECM at different spatial scales. The substrate is represented using viscoelastic elements, that is, Maxwell, Kelvin–Voigt, or standard linear solid (SLS) systems, parameterized by global substrate stiffness k_s', local substrate stiffness k_s, and clutch stiffness k_c. This formulation integrates the interplay between clutch loading, local ECM displacement, and time-dependent substrate relaxation (Liu et al. 2025).

nucleation, elongation, and Arp2/3 branching, allows retrograde flow to emerge naturally. By simulating thousands of stochastic clutches within two-dimensional networks, spatially resolved models capture heterogeneous force transmission, adhesion clustering, and stress fiber formation. This enables accurate predictions of filopodial extension, lamellipodial protrusion rates, adhesion distributions, and local traction peaks that match experiments (Campbell et al. 2023; Honasoge et al. 2023; Koser et al. 2016; Carney et al. 2023).

5.3.1 | Model of Growth Cone Mechanosensing

A recent extension of the motor-clutch framework explains mechanosensing in neuronal growth cones by incorporating stiffness-dependent clutch reinforcement (Pulido Cifuentes et al. 2024). This extension shows that local molecular rules scale up to specialized cellular structures. In this implementation, additional clutches are recruited when bonds experience forces above ~10 pN (Figure 4B), with the reinforcement rate tuned by substrate stiffness: $k_{add} = k_{add(0)} * \left(\sum_{i=1}^{n_{eng}} a(i) \right) * f_{available}$ where k_{add} is the rate of clutch addition, $k_{add(o)}$ is the optimized rate for a given stiffness (0.1–1 s^{-1}), n_{eng} is the number of engaged clutches at time t_k, $a(i)$ is 1 or 0 depending on whether the force on the clutch is greater than the force threshold, and $f_{available}$ is the fraction of clutches available for recruitment: $f_{available}(t_k) = \frac{n_{c,max} - n_c(t_k)}{n_{c,max}}$, where $n_{c,max}$ is the maximum number of clutches and $n_c(t_k)$ is the number available at time t_k. The model defines a functional transition point, where retrograde flow slows below 20 nm/s, as an approximation for strong cytoskeletal substrate coupling, corresponding to the transition of *Aplysia* growth cones from a state of slow advance and little/no substrate coupling to a state of fast advance and strong substrate coupling (Lin and Forscher 1995; Suter and Forscher 2001). Simulations start with an unloaded actin retrograde flow of 100 nm/s, and as clutches stochastically bind and unbind, they modulate actin flow, their own positions, and substrate displacement. Tension builds on engaged clutches, transmitting myosin-generated forces to the elastic substrate (k_{sub} = 0.05–2.5 kPa), enabling measurement of latency time and substrate deformation. Sensitivity analysis reveals a biphasic dependence of latency on substrate stiffness, with the fastest response on soft substrates (~0.1 kPa), consistent with microneedle experiments on *Aplysia* growth (Koser et al. 2016). While the parameters were tuned for *Aplysia* growth cones, mechanistic principles such as force-threshold recruitment, stiffness-dependent reinforcement, and retrograde flow readouts are broadly applicable to other adhesive systems that employ molecular clutch mechanics. Reparameterization is required for quantitative predictions in cells with differing cytoskeletal architecture, adhesion composition, myosin contractility, or size scale.

5.3.2 | Mechano-Chemical Adhesion Maturation

Other extensions of the motor-clutch framework incorporate mechano-chemical regulation of focal adhesion (FA) maturation (Honasoge et al. 2023). Ordinary differential equation-based models track integrin–talin–vinculin dynamics (Figure 4C), clustering, actin binding, and force-dependent unbinding while including reinforcement via talin unfolding. Nascent adhesions form as small "seeds" of integrin–adaptor complexes, which can dimerize into larger "clusts" (Figure 4C). Actin binding to talin enables force transmission and talin unfolding, exposing vinculin-binding sites for stepwise reinforcement to stronger complexes including up to 3 vinculin molecules. Signal-dependent and time-dependent rate modifications regulate assembly and disassembly based on experimentally captured adhesion formation and breakdown times (Chan and Odde 2008), while a Michaelis–Menten-based signaling decay prevents indefinite adhesion formation. Simulations with forward Euler integration over 600 s capture adhesion assembly, maturation, and traction force generation, demonstrating stiffness-dependent behavior, partial vinculin recruitment, and realistic FA maturation. Despite simplifications, this framework generalizes to diverse mechanotransduction systems and allows exploration of how molecular concentration, kinetics, or mechanochemical parameters influence adhesion dynamics.

5.3.3 | Differential Transmission Model

A differential transmission model, named for its analogy to a mechanical differential, lets connected components move at different rates while still transmitting force and explicitly incorporates non-linear adaptor-protein mechanics and local substrate

19493592, 0, Downloaded from https://onlinelibrary.wiley.com/doi/10.1002/cm.70221, Wiley Online Library on [25/11/2026]. See the Terms and Conditions (https://onlinelibrary.wiley.com/terms-and-conditions) on Wiley Online Library for rules of use; OA articles are governed by the applicable Creative Commons License

deformation (Liu et al. 2025). This framework demonstrates a conceptual shift from simple "load-and-fail" dynamics to multi-element composite mechanics, revealing that differential transmission and bistability arise inherently from the interplay between local substrate deformation and internal compliance. Each clutch is represented as a composite spring with intracellular (k_c), and extracellular (k_s') components. The mechanical system therefore contains three elastic elements: an intracellular clutch spring (k_c), a local substrate spring (k_s), and a larger-scale extracellular substrate spring (k_s') (Figure 4D). Substrate deformation dominates force transmission. The force–extension relation is:$F = k_{cl} l, with\ k_{cl} = \frac{k_c k_s}{k_c + k_s}$, where k_c is the intracellular spring constant and k_s the local substrate spring constant.

Clutch states are described by a probability distribution $p_{on}(l,t)$ satisfying: $p_{off}(t) + \int_{-\infty}^{+\infty} p_{on}(l,t)dl = 1$, with $p_{\text{off}}(t)$ denoting the probability of the off state. Clutch extensions can be positive or negative depending on their orientation. Non-linear elasticity, including protein unfolding thresholds, and substrate viscoelasticity (Maxwell, Kelvin–Voigt, or SLS models, Figure 4D), are incorporated. This framework predicts substrate-dependent steady states, force-loading rates, and fluctuation dynamics, revealing emergent behaviors such as differential transmission and bistability not captured by conventional load-and-fail models.

5.4 | Comparing Advances in the Molecular Clutch Framework

Progress in motor–clutch modeling reflects a systematic expansion of the physical and biochemical processes considered essential for mechanosensing. Early clutch models relied on load–fail dynamics in which identical, memoryless clutches resisted myosin-driven actin flow, reproducing biphasic traction–stiffness responses. Reinforcement-based models introduced stiffness-dependent recruitment of new load-bearing linkages. Mechano-chemical maturation frameworks further coupled integrin activation, talin unfolding, vinculin recruitment, and clutch clustering to local signaling. More recent differential-transmission models explicitly incorporate non-linear adaptor-protein elasticity and local substrate deformation.

Together, these developments trace a clear trajectory: from simple load–fail springs toward multiscale, history-dependent networks that integrate mechanical elasticity, biochemical transitions, reinforcement, and spatial heterogeneity. Modern models not only reproduce traction curves but also predict adhesion maturation, bistability, and stiffness-history effects, emphasizing that mechanosensing emerges from the collective behavior of coupled mechanical and biochemical clutch systems.

6 | Summary and Outlook

The cytoskeleton functions as a multiscale, dynamic network where atomic-level interactions dictate spatial organization, force transmission, and emergent cellular properties. As reviewed here, no single computational method can capture these processes across all spatiotemporal scales. Instead, a hierarchical modeling paradigm is required to fully resolve cytoskeletal behavior. AA MD simulations capture residue-level fluctuations, force-induced conformational changes, nucleotide-dependent transitions, and protein–protein interfaces, directly connecting static structural data from experiments or AI predictions to dynamic molecular behavior. To reach broader spatial and temporal scales, CG models group atomic degrees of freedom into effective interaction sites, making it possible to simulate filament-level mechanics, dynamic instability, curvature transitions, and supramolecular assemblies. At the highest level, mesoscale frameworks simplify macromolecular details to evaluate network-level phenomena, including network remodeling, cellular traction, force transmission, and cell–matrix coupling over micrometers and minutes. Together, these computational methods have provided critical insights into the coordinated functions of F-actin, MTs, and adhesion complexes that remain difficult or impossible to isolate experimentally.

Increasingly, AA MD simulations inform CG and mesoscale parameterization, while higher-level models motivate targeted molecular studies. ML approaches are accelerating this integration by enabling adaptive resolution, automated coarse-graining, and enhanced sampling. To date, many AA and CG simulation studies have focused on segments of MTs and F-actin, revealing their dynamic nature when isolated, while others have focused on MAPs and ABPs interacting with MTs and F-actin respectively, shedding light on their interaction surfaces. The remaining larger-scale modeling efforts span a diverse spectrum of physical resolutions and formalisms, including (i) BD simulations, (ii) 3D mechanochemical models, (iii) UCG models, and (iv) kMC models. Future work on multiscale and hybrid approaches may address: (i) the dynamic role of PTMs on the surface of MTs and F-actins while interacting with associated proteins and biochemical compounds, and whether they are potential targets for drug discovery; (ii) the mechanism of branching or bundling of cytoskeletal filaments (via cross-linking proteins) and their impact on (sub-)cellular activity; (iii) the significance and dynamics of MT doublet architectures (Tai et al. 2023; Liu et al. 2026) and the residence of F-actin within MT lumen, as revealed by cryo-ET studies (Ventura Santos et al. 2023; Paul et al. 2020; Tsuji et al. 2024); (iv) 3D meso-scale cellular models that contain sub-models of cytoskeletal filaments and simplified representations of proteins, where the growth/shrinkage of filaments and binding/unbinding of associated proteins stochastically follow kinetic rates. Computational studies have already begun to address these questions while leaving scope for more integrated multiscale approaches. For instance, (i) cryo-EM-guided MD has shown that α-tubulin K40 acetylation modifies the conformational ensemble of the αK40 loop and MT lateral interactions, while CG MD has demonstrated that tubulin PTMs can modulate dynein–MT interactions and motor behavior (Eshun-Wilson et al. 2019). Future simulations could incorporate combinations of PTMs together with MAPs, motors, and small molecules to determine how local PTM-dependent changes in molecular interactions propagate to MT or F-actin mechanics and to identify PTM-sensitive interfaces that may be pharmacologically targeted. Regarding F-actin branching

19493592, 0, Downloaded from https://onlinelibrary.wiley.com/doi/10.1002/cm.70221, Wiley Online Library on [25/11/2026]. See the Terms and Conditions (https://onlinelibrary.wiley.com/terms-and-conditions) on Wiley Online Library for rules of use; OA articles are governed by the applicable Creative Commons License

and bundling, AA and CG MD have resolved conformational transitions in Arp2/3-mediated branch nucleation, whereas mesoscale models have reproduced crosslinker- and motor-driven F-actin organization and bundling (Singh et al. 2023; Popov et al. 2016). Going forward, coupling molecular descriptions of individual cross-linking interfaces to larger F-actin network models could reveal how changes in binding energetics translate into F-actin network architecture and cellular mechanics. For MT doublets, CG MD has examined the mechanical stabilization of the A–B MT tubule outer junction by associated proteins, while hybrid cryo-EM/MD studies have investigated how tubulin acetylation influences doublet architecture (Kubo et al. 2023; Yang et al. 2024). Future models could address how doublet-specific MAPs, PTMs, and motor-generated forces collectively determine doublet deformation and function. Finally, mesoscale frameworks such as MEDYAN and Cytosim already represent dynamic cytoskeletal filaments, motors, and cross-linkers through combinations of stochastic kinetics, Brownian dynamics, and mechanical interactions (Popov et al. 2016; Freedman et al. 2017). A major next step is therefore to develop increasingly realistic three-dimensional cellular models in which F-actin and MT networks coexist and dynamically remodel while their kinetic and mechanical parameters are informed directly by finer-grained molecular simulations and experimental measurements. A further extension would be to more systematically couple MD-derived structural dynamics, interaction energies, mechanical forces, and strain to dynamically update kinetic rates within multi-scale cytoskeletal models. These insights from in silico approaches could substantially contribute to advancing our understanding of the cytoskeleton.

Overall, looking forward, key challenges will include unifying actin and MT models within shared cytoskeletal frameworks, coupling cytoskeletal mechanics to membrane deformation and 3D cell geometry, and directly constraining simulations with live-cell imaging data. ML approaches could play a key role in this integration by extracting quantitative information on cytoskeletal architecture, filament dynamics, cellular forces, and other model parameters from large imaging datasets, which could then be used to parameterize or iteratively constrain mechanistic simulations. Recent studies have, for example, used ML to reconstruct individual F-actin networks from live-cell imaging and neural networks to infer cellular mechanical forces directly from images of cytoskeletal-associated proteins (Ju et al. 2024; Schmitt et al. 2024). Continued development of transferable force fields, physics-informed ML approaches (Ahmadi et al. 2026), and adaptive multiscale algorithms, where fine-grained molecular detail is preserved in some regions of interest in a simulated system while the rest of the system is simulated at a lower resolution, will be essential for achieving predictive, cross-scale models of cytoskeletal organization, force transmission, and mechanotransduction.

Funding

This work was supported by the National Institute of General Medical Sciences (NIGMS) of the National Institutes of Health under grant number R35GM147491.

Conflicts of Interest

The authors declare no conflicts of interest.

Data Availability Statement

Data sharing not applicable to this article as no datasets were generated or analyzed during the current study.

References

Abramson, J., J. Adler, J. Dunger, et al. 2024. "Addendum: Accurate Structure Prediction of Biomolecular Interactions With AlphaFold 3." *Nature* 636: E4. https://doi.org/10.1038/s41586-024-08416-7.

Ahmadi, N., Q. Cao, J. D. Humphrey, and G. E. Karniadakis. 2026. "Physics-Informed Machine Learning in Biomedical Science and Engineering." *Annual Review of Biomedical Engineering* 28: 309–336. https://doi.org/10.1146/annurev-bioeng-110824-124907.

Al-Bassam, J., R. S. Ozer, D. Safer, S. Halpain, and R. A. Milligan. 2002. "MAP2 and Tau Bind Longitudinally Along the Outer Ridges of Microtubule Protofilaments." *Journal of Cell Biology* 157: 1187–1196. https://doi.org/10.1083/jcb.200201048.

Alexandrova, V. V., M. N. Anisimov, A. V. Zaitsev, et al. 2022. "Theory of Tip Structure-Dependent Microtubule Catastrophes and Damage-Induced Microtubule Rescues." *Proceedings of the National Academy of Sciences of the United States of America* 119: e2208294119. https://doi.org/10.1073/pnas.2208294119.

Alonso-Matilla, R., P. P. Provenzano, and D. J. Odde. 2023. "Optimal Cell Traction Forces in a Generalized Motor-Clutch Model." *Biophysical Journal* 122: 3369–3385. https://doi.org/10.1016/j.bpj.2023.07.012.

Alushin, G. M., G. C. Lander, E. H. Kellogg, et al. 2014. "High-Resolution Microtubule Structures Reveal the Structural Transitions in Alphabeta-Tubulin Upon GTP Hydrolysis." *Cell* 157: 1117–1129. https://doi.org/10.1016/j.cell.2014.03.053.

Andreu, I., B. Falcones, S. Hurst, et al. 2021. "The Force Loading Rate Drives Cell Mechanosensing Through Both Reinforcement and Cytoskeletal Softening." *Nature Communications* 12: 4229. https://doi.org/10.1038/s41467-021-24383-3.

Atherton, J., M. Stouffer, F. Francis, and C. A. Moores. 2018. "Microtubule Architecture In Vitro and in Cells Revealed by Cryo-Electron Tomography." *Acta Crystallographica Section D, Structural Biology* 74: 572–584. https://doi.org/10.1107/S2059798318001948.

Badaczewska-Dawid, A. E., A. Kolinski, and S. Kmiecik. 2020. "Computational Reconstruction of Atomistic Protein Structures From Coarse-Grained Models." *Computational and Structural Biotechnology Journal* 18: 162–176. https://doi.org/10.1016/j.csbj.2019.12.007.

Baek, M., F. DiMaio, I. Anishchenko, et al. 2021. "Accurate Prediction of Protein Structures and Interactions Using a Three-Track Neural Network." *Science* 373: 871–876. https://doi.org/10.1126/science.abj8754.

Bangasser, B. L., S. S. Rosenfeld, and D. J. Odde. 2013. "Determinants of Maximal Force Transmission in a Motor-Clutch Model of Cell Traction in a Compliant Microenvironment." *Biophysical Journal* 105: 581–592. https://doi.org/10.1016/j.bpj.2013.06.027.

Bangasser, B. L., G. A. Shamsan, C. E. Chan, et al. 2017. "Shifting the Optimal Stiffness for Cell Migration." *Nature Communications* 8: 15313. https://doi.org/10.1038/ncomms15313.

Barducci, A., M. Bonomi, and M. Parrinello. 2011. "Metadynamics." *WIREs Computational Molecular Science* 1: 826–843. https://doi.org/10.1002/wcms.31.

Bareja, I., O. Kučera, I. I. Petitjean, et al. 2025. "Anillin Directly Crosslinks Microtubules With Actin Filaments." *EMBO Journal* 44: 4803–4824. https://doi.org/10.1038/s44318-025-00492-3.

19493592, 0, Downloaded from https://onlinelibrary.wiley.com/doi/10.1002/cm.70221, Wiley Online Library on [25/11/2026]. See the Terms and Conditions (https://onlinelibrary.wiley.com/terms-and-conditions) on Wiley Online Library for rules of use; OA articles are governed by the applicable Creative Commons License

Beckett, D., and G. A. Voth. 2023. "Unveiling the Catalytic Mechanism of GTP Hydrolysis in Microtubules." *Proceedings of the National Academy of Sciences of the United States of America* 120: e2305899120. https://doi.org/10.1073/pnas.2305899120.

Bell, G. I. 1978. "Models for the Specific Adhesion of Cells to Cells." *Science* 200: 618–627. https://doi.org/10.1126/science.347575.

Bernardi, R. C., M. C. R. Melo, and K. Schulten. 2015. "Enhanced Sampling Techniques in Molecular Dynamics Simulations of Biological Systems." *Biochimica et Biophysica Acta* 1850: 872–877. https://doi.org/10.1016/j.bbagen.2014.10.019.

Bezanilla, M., A. S. Gladfelter, D. R. Kovar, and W. L. Lee. 2015. "Cytoskeletal Dynamics: A View From the Membrane." *Journal of Cell Biology* 209: 329–337. https://doi.org/10.1083/jcb.201502062.

Bidone, T. C., W. Jung, D. Maruri, C. Borau, R. D. Kamm, and T. Kim. 2017. "Morphological Transformation and Force Generation of Active Cytoskeletal Networks." *PLoS Computational Biology* 13: e1005277. https://doi.org/10.1371/journal.pcbi.1005277.

Bidone, T. C., and D. J. Odde. 2023. "Multiscale Models of Integrins and Cellular Adhesions." *Current Opinion in Structural Biology* 80: 102576. https://doi.org/10.1016/j.sbi.2023.102576.

Bidone, T. C., H. Tang, and D. Vavylonis. 2014. "Dynamic Network Morphology and Tension Buildup in a 3D Model of Cytokinetic Ring Assembly." *Biophysical Journal* 107: 2618–2628. https://doi.org/10.1016/j.bpj.2014.10.034.

Binder, J., M. Zalar, M. Huelsmeyer, M. Siedler, R. Curtis, and W. Friess. 2025. "Enhancing Martini 3 for Protein Self-Interaction Simulations." *European Journal of Pharmaceutical Sciences* 209: 107068. https://doi.org/10.1016/j.ejps.2025.107068.

Blanchoin, L., R. Boujemaa-Paterski, C. Sykes, and J. Plastino. 2014. "Actin Dynamics, Architecture, and Mechanics in Cell Motility." *Physiological Reviews* 94: 235–263. https://doi.org/10.1152/physrev.00018.2013.

Borau, C., T. Kim, T. Bidone, J. M. Garcia-Aznar, and R. D. Kamm. 2012. "Dynamic Mechanisms of Cell Rigidity Sensing: Insights From a Computational Model of Actomyosin Networks." *PLoS One* 7: e49174. https://doi.org/10.1371/journal.pone.0049174.

Burdyniuk, M., A. Callegari, M. Mori, F. Nedelec, and P. Lenart. 2018. "F-Actin Nucleated on Chromosomes Coordinates Their Capture by Microtubules in Oocyte Meiosis." *Journal of Cell Biology* 217: 2661–2674. https://doi.org/10.1083/jcb.201802080.

Cabrales Fontela, Y., H. Kadavath, J. Biernat, D. Riedel, E. Mandelkow, and M. Zweckstetter. 2017. "Multivalent Cross-Linking of Actin Filaments and Microtubules Through the Microtubule-Associated Protein Tau." *Nature Communications* 8: 1981. https://doi.org/10.1038/s41467-017-02230-8.

Campbell, S., M. C. Mendoza, A. Rammohan, M. E. McKenzie, and T. C. Bidone. 2023. "Computational Model of Integrin Adhesion Elongation Under an Actin Fiber." *PLoS Computational Biology* 19: e1011237. https://doi.org/10.1371/journal.pcbi.1011237.

Cannariato, M., E. A. Zizzi, J. A. Tuszynski, and M. A. Deriu. 2024. "Multiscale Computational Analysis of the Effect of Taxol on Microtubule Mechanics." *ACS Biomaterials Science and Engineering* 10: 5666–5674. https://doi.org/10.1021/acsbiomaterials.4c00847.

Carney, K. R., A. M. Khan, S. Stam, et al. 2023. "Nascent Adhesions Shorten the Period of Lamellipodium Protrusion Through the Brownian Ratchet Mechanism." *Molecular Biology of the Cell* 34: ar115. https://doi.org/10.1091/mbc.E23-08-0314.

Castro, T. G., T. Ferreira, T. Matama, F. D. Munteanu, and A. Cavaco-Paulo. 2023. "Acetylation and Phosphorylation Processes Modulate Tau's Binding to Microtubules: A Molecular Dynamics Study." *Biochimica et Biophysica Acta—General Subjects* 1867: 130276. https://doi.org/10.1016/j.bbagen.2022.130276.

Chakraborty, S., M. Jasnin, and W. Baumeister. 2020. "Three-Dimensional Organization of the Cytoskeleton: A Cryo-Electron Tomography Perspective." *Protein Science* 29: 1302–1320. https://doi.org/10.1002/pro.3858.

Chan, C. E., and D. J. Odde. 2008. "Traction Dynamics of Filopodia on Compliant Substrates." *Science* 322: 1687–1691. https://doi.org/10.1126/science.1163595.

Chandrasekaran, A., K. Graham, J. C. Stachowiak, and P. Rangamani. 2024. "Kinetic Trapping Organizes Actin Filaments Within Liquid-Like Protein Droplets." *Nature Communications* 15: 3139. https://doi.org/10.1038/s41467-024-46726-6.

Chandrasekaran, A., A. Upadhyaya, and G. A. Papoian. 2019. "Remarkable Structural Transformations of Actin Bundles Are Driven by Their Initial Polarity, Motor Activity, Crosslinking, and Filament Treadmilling." *PLoS Computational Biology* 15: e1007156. https://doi.org/10.1371/journal.pcbi.1007156.

Chang, A. C., A. H. Mekhdjian, M. Morimatsu, A. K. Denisin, B. L. Pruitt, and A. R. Dunn. 2016. "Single Molecule Force Measurements in Living Cells Reveal a Minimally Tensioned Integrin State." *ACS Nano* 10: 10745–10752. https://doi.org/10.1021/acsnano.6b03314.

Chen, Y., J. Brasch, O. J. Harrison, and T. C. Bidone. 2021. "Computational Model of E-Cadherin Clustering Under Force." *Biophysical Journal* 120: 4944–4954. https://doi.org/10.1016/j.bpj.2021.10.018.

Chen, Y., and J. Yang. 2025. "Acceleration of the GROMACS Free-Energy Perturbation Calculations on GPUs." *ACS Omega* 10: 22858–22873. https://doi.org/10.1021/acsomega.5c00151.

Chen, Z., G. A. Greenan, M. Shiozaki, et al. 2023. "In Situ Cryo-Electron Tomography Reveals the Asymmetric Architecture of Mammalian Sperm Axonemes." *Nature Structural and Molecular Biology* 30: 360–369. https://doi.org/10.1038/s41594-022-00861-0.

Chen, Z., M. Shiozaki, K. M. Haas, et al. 2023. "De Novo Protein Identification in Mammalian Sperm Using In Situ Cryoelectron Tomography and AlphaFold2 Docking." *Cell* 186: 5041–5053.e5019. https://doi.org/10.1016/j.cell.2023.09.017.

Chirasani, V. R., M. A. I. Khan, J. N. Malavade, N. V. Dokholyan, B. D. Hoffman, and S. L. Campbell. 2023. "Molecular Basis and Cellular Functions of Vinculin-Actin Directional Catch Bonding." *Nature Communications* 14: 8300. https://doi.org/10.1038/s41467-023-43779-x.

Chou, S. Z., and T. D. Pollard. 2019. "Mechanism of Actin Polymerization Revealed by Cryo-EM Structures of Actin Filaments With Three Different Bound Nucleotides." *Proceedings of the National Academy of Sciences of the United States of America* 116: 4265–4274. https://doi.org/10.1073/pnas.1807028115.

Chu, J. W., and G. A. Voth. 2005. "Allostery of Actin Filaments: Molecular Dynamics Simulations and Coarse-Grained Analysis." *Proceedings of the National Academy of Sciences of the United States of America* 102: 13111–13116. https://doi.org/10.1073/pnas.0503732102.

Chu, J. W., and G. A. Voth. 2006. "Coarse-Grained Modeling of the Actin Filament Derived From Atomistic-Scale Simulations." *Biophysical Journal* 90: 1572–1582. https://doi.org/10.1529/biophysj.105.073924.

Cortes, D. B., M. Gordon, F. Nedelec, and A. S. Maddox. 2020. "Bond Type and Discretization of Nonmuscle Myosin II Are Critical for Simulated Contractile Dynamics." *Biophysical Journal* 118: 2703–2717. https://doi.org/10.1016/j.bpj.2020.03.033.

Dalhaimer, P., and T. D. Pollard. 2010. "Molecular Dynamics Simulations of Arp2/3 Complex Activation." *Biophysical Journal* 99: 2568–2576. https://doi.org/10.1016/j.bpj.2010.08.027.

Dama, J. F., M. Parrinello, and G. A. Voth. 2014. "Well-Tempered Metadynamics Converges Asymptotically." *Physical Review Letters* 112: 240602. https://doi.org/10.1103/PhysRevLett.112.240602.

De Simone, A., F. Nedelec, and P. Gonczy. 2016. "Dynein Transmits Polarized Actomyosin Cortical Flows to Promote Centrosome

19493592, 0, Downloaded from https://onlinelibrary.wiley.com/doi/10.1002/cm.70221, Wiley Online Library on [25/11/2026]. See the Terms and Conditions (https://onlinelibrary.wiley.com/terms-and-conditions) on Wiley Online Library for rules of use; OA articles are governed by the applicable Creative Commons License

Separation." *Cell Reports* 14: 2250–2262. https://doi.org/10.1016/j.celrep.2016.01.077.

Demosthene, B., M. Lee, R. R. Marracino, J. B. Heidings, and E. H. Kang. 2023. "Molecular Basis for Actin Polymerization Kinetics Modulated by Solution Crowding." *Biomolecules* 13: 786. https://doi.org/10.3390/biom13050786.

Deriu, M. A., T. C. Bidone, G. Grasso, A. Acquaviva, and U. Morbiducci. 2012. "Multiscale Modeling of Microtubules and Actin Filaments." *IFAC Proceedings Volumes* 45: 1023–1028. https://doi.org/10.3182/20120215-3-AT-3016.00181.

Deriu, M. A., T. C. Bidone, F. Mastrangelo, et al. 2011. "Biomechanics of Actin Filaments: A Computational Multi-Level Study." *Journal of Biomechanics* 44: 630–636. https://doi.org/10.1016/j.jbiomech.2010.11.014.

Desai, A., and T. J. Mitchison. 1997. "Microtubule Polymerization Dynamics." *Annual Review of Cell and Developmental Biology* 13: 83–117. https://doi.org/10.1146/annurev.cellbio.13.1.83.

Descovich, C. P., D. B. Cortes, S. Ryan, et al. 2018. "Cross-Linkers Both Drive and Brake Cytoskeletal Remodeling and Furrowing in Cytokinesis." *Molecular Biology of the Cell* 29: 622–631. https://doi.org/10.1091/mbc.E17-06-0392.

Ding, B., H. Y. Narvaez-Ortiz, Y. Singh, G. M. Hocky, S. Chowdhury, and B. J. Nolen. 2022. "Structure of Arp2/3 Complex at a Branched Actin Filament Junction Resolved by Single-Particle Cryo-Electron Microscopy." *Proceedings of the National Academy of Sciences of the United States of America* 119: e2202723119. https://doi.org/10.1073/pnas.2202723119.

Doga, H., B. Raubenolt, F. Cumbo, et al. 2024. "A Perspective on Protein Structure Prediction Using Quantum Computers." *Journal of Chemical Theory and Computation* 20: 3359–3378. https://doi.org/10.1021/acs.jctc.4c00067.

Dogterom, M., and G. H. Koenderink. 2019. "Actin-Microtubule Crosstalk in Cell Biology." *Nature Reviews. Molecular Cell Biology* 20: 38–54. https://doi.org/10.1038/s41580-018-0067-1.

Elosegui-Artola, A., E. Bazellières, M. D. Allen, et al. 2014. "Rigidity Sensing and Adaptation Through Regulation of Integrin Types." *Nature Materials* 13: 631–637. https://doi.org/10.1038/nmat3960.

Elosegui-Artola, A., R. Oria, Y. Chen, et al. 2016. "Mechanical Regulation of a Molecular Clutch Defines Force Transmission and Transduction in Response to Matrix Rigidity." *Nature Cell Biology* 18: 540–548. https://doi.org/10.1038/ncb3336.

Elosegui-Artola, A., X. Trepat, and P. Roca-Cusachs. 2018. "Control of Mechanotransduction by Molecular Clutch Dynamics." *Trends in Cell Biology* 28: 356–367. https://doi.org/10.1016/j.tcb.2018.01.008.

Eshun-Wilson, L., R. Zhang, D. Portran, et al. 2019. "Effects of Alpha-Tubulin Acetylation on Microtubule Structure and Stability." *Proceedings of the National Academy of Sciences of the United States of America* 116: 10366–10371. https://doi.org/10.1073/pnas.1900441116.

Feng, Y., and S. Mitran. 2018. "Data-Driven Reduced-Order Model of Microtubule Mechanics." *Cytoskeleton (Hoboken)* 75: 45–60. https://doi.org/10.1002/cm.21419.

Fisher, T. E., A. F. Oberhauser, M. Carrion-Vazquez, P. E. Marszalek, and J. M. Fernandez. 1999. "The Study of Protein Mechanics With the Atomic Force Microscope." *Trends in Biochemical Sciences* 24: 379–384. https://doi.org/10.1016/s0968-0004(99)01453-x.

Fletcher, D. A., and R. D. Mullins. 2010. "Cell Mechanics and the Cytoskeleton." *Nature* 463: 485–492. https://doi.org/10.1038/nature08908.

Freedman, S. L., S. Banerjee, G. M. Hocky, and A. R. Dinner. 2017. "A Versatile Framework for Simulating the Dynamic Mechanical Structure of Cytoskeletal Networks." *Biophysical Journal* 113: 448–460. https://doi.org/10.1016/j.bpj.2017.06.003.

Gardner, M. K., B. D. Charlebois, I. M. Jánosi, J. Howard, A. J. Hunt, and D. J. Odde. 2011. "Rapid Microtubule Self-Assembly Kinetics." *Cell* 146: 582–592. https://doi.org/10.1016/j.cell.2011.06.053.

Gardner, M. K., M. Zanic, and J. Howard. 2013. "Microtubule Catastrophe and Rescue." *Current Opinion in Cell Biology* 25: 14–22. https://doi.org/10.1016/j.ceb.2012.09.006.

Ghanta, K. P., J. C. Tardiff, and S. D. Schwartz. 2025. "Unraveling Mutation-Induced Protein Communication Pathways in the Actomyosin Complex: Insights From Comprehensive Metadynamics Simulations." *Journal of Physical Chemistry. B* 129: 8868–8879. https://doi.org/10.1021/acs.jpcb.5c02978.

Gibeaux, R., A. Z. Politi, P. Philippsen, and F. Nedelec. 2017. "Mechanism of Nuclear Movements in a Multinucleated Cell." *Molecular Biology of the Cell* 28: 645–660. https://doi.org/10.1091/mbc.E16-11-0806.

Gill, M., and M. E. McCully. 2019. "Molecular Dynamics Simulations Suggest Stabilizing Mutations in a De Novo Designed Alpha/Beta Protein." *Protein Engineering, Design and Selection* 32: 317–329. https://doi.org/10.1093/protein/gzaa005.

Gong, R., M. J. Reynolds, K. R. Carney, K. Hamilton, T. C. Bidone, and G. M. Alushin. 2025. "Fascin Structural Plasticity Mediates Flexible Actin Bundle Construction." *Nature Structural and Molecular Biology* 32: 940–952. https://doi.org/10.1038/s41594-024-01477-2.

Gong, Z., S. E. Szczesny, S. R. Caliari, et al. 2018. "Matching Material and Cellular Timescales Maximizes Cell Spreading on Viscoelastic Substrates." *Proceedings of the National Academy of Sciences of the United States of America* 115: E2686–E2695. https://doi.org/10.1073/pnas.1716620115.

Grudtsyna, V., S. Packirisamy, T. C. Bidone, and V. Swaminathan. 2023. "Extracellular Matrix Sensing via Modulation of Orientational Order of Integrins and F-Actin in Focal Adhesions." *Life Science Alliance* 6: e202301898. https://doi.org/10.26508/lsa.202301898.

Gudimchuk, N. B., E. V. Ulyanov, E. O'Toole, et al. 2020. "Mechanisms of Microtubule Dynamics and Force Generation Examined With Computational Modeling and Electron Cryotomography." *Nature Communications* 11: 3765. https://doi.org/10.1038/s41467-020-17553-2.

Guo, W., T. A. Ale, S. Sun, J. E. Sanchez, and L. Li. 2023. "A Comprehensive Study on the Electrostatic Properties of Tubulin-Tubulin Complexes in Microtubules." *Cells* 12: 238. https://doi.org/10.3390/cells12020238.

Guo, W., D. du, H. Zhang, et al. 2024. "Bound Ion Effects: Using Machine Learning Method to Study the Kinesin Ncd's Binding With Microtubule." *Biophysical Journal* 123: 2740–2748. https://doi.org/10.1016/j.bpj.2023.12.024.

Harker, A. J., H. H. Katkar, T. C. Bidone, et al. 2019. "Ena/VASP Processive Elongation Is Modulated by Avidity on Actin Filaments Bundled by the Filopodia Cross-Linker Fascin." *Molecular Biology of the Cell* 30: 851–862. https://doi.org/10.1091/mbc.E18-08-0500.

Havelka, D., M. A. Deriu, M. Cifra, and O. Kucera. 2017. "Deformation Pattern in Vibrating Microtubule: Structural Mechanics Study Based on an Atomistic Approach." *Scientific Reports* 7: 4227. https://doi.org/10.1038/s41598-017-04272-w.

Hemmat, M., and D. J. Odde. 2021. "Atomistic Basis of Microtubule Dynamic Instability Assessed via Multiscale Modeling." *Annals of Biomedical Engineering* 49: 1716–1734. https://doi.org/10.1007/s10439-020-02715-6.

Hirata, H., H. Tatsumi, C. T. Lim, and M. Sokabe. 2014. "Force-Dependent Vinculin Binding to Talin in Live Cells: A Crucial Step in Anchoring the Actin Cytoskeleton to Focal Adhesions." *American Journal of Physiology. Cell Physiology* 306: C607–C620. https://doi.org/10.1152/ajpcell.00122.2013.

19493592, 0, Downloaded from https://onlinelibrary.wiley.com/doi/10.1002/cm.70221, Wiley Online Library on [25/11/2026]. See the Terms and Conditions (https://onlinelibrary.wiley.com/terms-and-conditions) on Wiley Online Library for rules of use; OA articles are governed by the applicable Creative Commons License

Holehouse, A. S., and B. B. Kragelund. 2024. "The Molecular Basis for Cellular Function of Intrinsically Disordered Protein Regions." *Nature Reviews. Molecular Cell Biology* 25: 187–211. https://doi.org/10.1038/s41580-023-00673-0.

Honasoge, K. S., Z. Karagöz, B. T. Goult, H. Wolfenson, V. L. S. LaPointe, and A. Carlier. 2023. "Force-Dependent Focal Adhesion Assembly and Disassembly: A Computational Study." *PLoS Computational Biology* 19: e1011500. https://doi.org/10.1371/journal.pcbi.1011500.

Huang, D. L., N. A. Bax, C. D. Buckley, W. I. Weis, and A. R. Dunn. 2017. "Vinculin Forms a Directionally Asymmetric Catch Bond With F-Actin." *Science* 357: 703–706. https://doi.org/10.1126/science.aan2556.

Huang, J., S. Rauscher, G. Nawrocki, et al. 2017. "CHARMM36m: An Improved Force Field for Folded and Intrinsically Disordered Proteins." *Nature Methods* 14: 71–73. https://doi.org/10.1038/nmeth.4067.

Igaev, M., and H. Grubmuller. 2022. "Bending-Torsional Elasticity and Energetics of the Plus-End Microtubule Tip." *Proceedings of the National Academy of Sciences of the United States of America* 119: e2115516119. https://doi.org/10.1073/pnas.2115516119.

Inaba, H., T. Imasaki, K. Aoyama, et al. 2025. "Cryo-ET of Actin Cytoskeleton and Membrane Structure in Lamellipodia Formation Using Optogenetics." *iScience* 28: 112529. https://doi.org/10.1016/j.isci.2025.112529.

Isomursu, A., K. Y. Park, J. Hou, et al. 2022. "Directed Cell Migration Towards Softer Environments." *Nature Materials* 21: 1081–1090. https://doi.org/10.1038/s41563-022-01294-2.

Ju, H., H. Skibbe, M. Fukui, S. H. Yoshimura, and H. Naoki. 2024. "Machine Learning-Guided Reconstruction of Cytoskeleton Network From Live-Cell AFM Images." *iScience* 27: 110907. https://doi.org/10.1016/j.isci.2024.110907.

Jumper, J., R. Evans, A. Pritzel, et al. 2021. "Highly Accurate Protein Structure Prediction With AlphaFold." *Nature* 596: 583–589. https://doi.org/10.1038/s41586-021-03819-2.

Kalutskii, M., H. Grubmuller, V. A. Volkov, and M. Igaev. 2025. "Microtubule Dynamics Are Defined by Conformations and Stability of Clustered Protofilaments." *Proceedings of the National Academy of Sciences of the United States of America* 122: e2424263122. https://doi.org/10.1073/pnas.2424263122.

Kaminski, G. A., R. A. Friesner, J. Tirado-Rives, and W. L. Jorgensen. 2001. "Evaluation and Reparametrization of the OPLS-AA Force Field for Proteins via Comparison With Accurate Quantum Chemical Calculations on Peptides." *Journal of Physical Chemistry B* 105: 6474–6487. https://doi.org/10.1021/jp003919d.

Kim, T. 2015. "Determinants of Contractile Forces Generated in Disorganized Actomyosin Bundles." *Biomechanics and Modeling in Mechanobiology* 14: 345–355. https://doi.org/10.1007/s10237-014-0608-2.

Kim, T., W. Hwang, and R. D. Kamm. 2009. "Computational Analysis of a Cross-Linked Actin-Like Network." *Experimental Mechanics* 49: 91–104. https://doi.org/10.1007/s11340-007-9091-3.

Kim, T., W. Hwang, H. Lee, and R. D. Kamm. 2009. "Computational Analysis of Viscoelastic Properties of Crosslinked Actin Networks." *PLoS Computational Biology* 5: e1000439. https://doi.org/10.1371/journal.pcbi.1000439.

Kondratyuk, N., V. Nikolskiy, D. Pavlov, and V. Stegailov. 2021. "GPU-Accelerated Molecular Dynamics: State-Of-Art Software Performance and Porting From Nvidia CUDA to AMD HIP." *International Journal of High Performance Computing Applications* 35: 312–324. https://doi.org/10.1177/10943420211008288.

Kong, F., A. J. Garcia, A. P. Mould, M. J. Humphries, and C. Zhu. 2009. "Demonstration of Catch Bonds Between an Integrin and Its Ligand." *Journal of Cell Biology* 185: 1275–1284. https://doi.org/10.1083/jcb.200810002.

Koser, D. E., A. J. Thompson, S. K. Foster, et al. 2016. "Mechanosensing Is Critical for Axon Growth in the Developing Brain." *Nature Neuroscience* 19: 1592–1598. https://doi.org/10.1038/nn.4394.

Kroon, P. C., F. Grünewald, J. Barnoud, et al. 2025. "Martinize2 and Vermouth Provide a Unified Framework for Molecular Topology Generation." *eLife* 12: RP90627. https://doi.org/10.7554/eLife.90627.

Kubo, S., C. S. Black, E. Joachimiak, et al. 2023. "Native Doublet Microtubules From Tetrahymena Thermophila Reveal the Importance of Outer Junction Proteins." *Nature Communications* 14: 2168. https://doi.org/10.1038/s41467-023-37868-0.

Kutzner, C., S. Páll, M. Fechner, A. Esztermann, B. L. de Groot, and H. Grubmüller. 2015. "Best Bang for Your Buck: GPU Nodes for GROMACS Biomolecular Simulations." *Journal of Computational Chemistry* 36: 1990–2008. https://doi.org/10.1002/jcc.24030.

Laio, A., and M. Parrinello. 2002. "Escaping Free-Energy Minima." *Proceedings of the National Academy of Sciences of the United States of America* 99: 12562–12566. https://doi.org/10.1073/pnas.202427399.

Laporte, S., and A. Magistrato. 2021. "Deciphering the Molecular Terms of Arp2/3 Allosteric Regulation From All-Atom Simulations and Dynamical Network Theory." *Journal of Physical Chemistry Letters* 12: 5384–5389. https://doi.org/10.1021/acs.jpclett.1c00940.

Lehman, W., X. Li, F. A. Kiani, et al. 2018. "Precise Binding of Tropomyosin on Actin Involves Sequence-Dependent Variance in Coiled-Coil Twisting." *Biophysical Journal* 115: 1082–1092. https://doi.org/10.1016/j.bpj.2018.08.017.

Li, S., J. Zhang, C. Wang, and P. Nithiarasu. 2018. "Atomistic Modeling of F-Actin Mechanical Responses and Determination of Mechanical Properties." *ACS Biomaterials Science and Engineering* 4: 2794–2803. https://doi.org/10.1021/acsbiomaterials.8b00640.

Li, X., Q. Ni, X. He, et al. 2020. "Tensile Force-Induced Cytoskeletal Remodeling: Mechanics Before Chemistry." *PLoS Computational Biology* 16: e1007693. https://doi.org/10.1371/journal.pcbi.1007693.

Liman, J., C. Bueno, Y. Eliaz, et al. 2020. "The Role of the Arp2/3 Complex in Shaping the Dynamics and Structures of Branched Actomyosin Networks." *Proceedings of the National Academy of Sciences of the United States of America* 117: 10825–10831. https://doi.org/10.1073/pnas.1922494117.

Lin, C. H., and P. Forscher. 1995. "Growth Cone Advance Is Inversely Proportional to Retrograde F-Actin Flow." *Neuron* 14: 763–771. https://doi.org/10.1016/0896-6273(95)90220-1.

Lindorff-Larsen, K., S. Piana, K. Palmo, et al. 2010. "Improved Side-Chain Torsion Potentials for the Amber ff99SB Protein Force Field." *Proteins* 78: 1950–1958. https://doi.org/10.1002/prot.22711.

Liu, P., Q. Wang, X. Dai, et al. 2025. "Elastic Properties of Force-Transmitting Linkages Determine Multistable Mechanosensitive Behaviour of Cell Adhesion." *Nature Physics* 21: 1431–1443. https://doi.org/10.1038/s41567-025-02964-z.

Liu, Q., L. Zhou, X. Liang, et al. 2026. "Doublet Microtubule-Associated Tektins and Enzymes Differentially Regulate Sperm Flagellar Integrity and Motility." *Nature Communications* 17: 3316. https://doi.org/10.1038/s41467-026-69714-4.

Lombardi, L. E., M. A. Marti, and L. Capece. 2016. "CG2AA: Backmapping Protein Coarse-Grained Structures." *Bioinformatics* 32: 1235–1237. https://doi.org/10.1093/bioinformatics/btv740.

Loughlin, R., R. Heald, and F. Nedelec. 2010. "A Computational Model Predicts Xenopus Meiotic Spindle Organization." *Journal of Cell Biology* 191: 1239–1249. https://doi.org/10.1083/jcb.201006076.

Louison, K. A., I. L. Dryden, and C. A. Laughton. 2021. "GLIMPS: A Machine Learning Approach to Resolution Transformation for Multiscale Modeling." *Journal of Chemical Theory and Computation* 17: 7930–7937. https://doi.org/10.1021/acs.jctc.1c00735.

19493592, 0, Downloaded from https://onlinelibrary.wiley.com/doi/10.1002/cm.70221, Wiley Online Library on [25/11/2026]. See the Terms and Conditions (https://onlinelibrary.wiley.com/terms-and-conditions) on Wiley Online Library for rules of use; OA articles are governed by the applicable Creative Commons License

Lyman, E., J. Pfaendtner, and G. A. Voth. 2008. "Systematic Multiscale Parameterization of Heterogeneous Elastic Network Models of Proteins." *Biophysical Journal* 95: 4183–4192. https://doi.org/10.1529/biophysj.108.139733.

MacTaggart, B., and A. Kashina. 2021. "Posttranslational Modifications of the Cytoskeleton." *Cytoskeleton* 78: 142–173. https://doi.org/10.1002/cm.21679.

Margolin, G., I. V. Gregoretti, T. M. Cickovski, et al. 2012. "The Mechanisms of Microtubule Catastrophe and Rescue: Implications From Analysis of a Dimer-Scale Computational Model." *Molecular Biology of the Cell* 23: 642–656. https://doi.org/10.1091/mbc.E11-08-0688.

Marrink, S. J., L. Monticelli, M. N. Melo, R. Alessandri, D. P. Tieleman, and P. C. T. Souza. 2023. "Two Decades of Martini: Better Beads, Broader Scope." *WIREs Computational Molecular Science* 13: e1620. https://doi.org/10.1002/wcms.1620.

Marrink, S. J., H. J. Risselada, S. Yefimov, D. P. Tieleman, and A. H. de Vries. 2007. "The MARTINI Force Field: Coarse Grained Model for Biomolecular Simulations." *Journal of Physical Chemistry. B* 111: 7812–7824. https://doi.org/10.1021/jp071097f.

McIntosh, J. R., E. O'Toole, G. Morgan, et al. 2018. "Microtubules Grow by the Addition of Bent Guanosine Triphosphate Tubulin to the Tips of Curved Protofilaments." *Journal of Cell Biology* 217: 2691–2708. https://doi.org/10.1083/jcb.201802138.

Mehdi, S., Z. Smith, L. Herron, Z. Zou, and P. Tiwary. 2024. "Enhanced Sampling With Machine Learning." *Annual Review of Physical Chemistry* 75: 347–370. https://doi.org/10.1146/annurev-physchem-083122-125941.

Mohan, R., and A. John. 2015. "Microtubule-Associated Proteins as Direct Crosslinkers of Actin Filaments and Microtubules." *IUBMB Life* 67: 395–403. https://doi.org/10.1002/iub.1384.

Molloy, J. E., J. E. Burns, J. Kendrick-Jones, R. T. Tregear, and D. C. White. 1995. "Movement and Force Produced by a Single Myosin Head." *Nature* 378: 209–212. https://doi.org/10.1038/378209a0.

Mukadum, F., W. J. Pena Ccoa, and G. M. Hocky. 2024. "Molecular Simulation Approaches to Probing the Effects of Mechanical Forces in the Actin Cytoskeleton." *Cytoskeleton (Hoboken)* 81: 318–327. https://doi.org/10.1002/cm.21837.

Nasedkin, A., I. Ermilova, and J. Swenson. 2021. "Atomistic Molecular Dynamics Simulations of Tubulin Heterodimers Explain the Motion of a Microtubule." *European Biophysics Journal* 50: 927–940. https://doi.org/10.1007/s00249-021-01553-1.

Nasrin, S. R., T. Yamashita, M. Ikeguchi, et al. 2024. "Tensile Stress on Microtubules Facilitates Dynein-Driven Cargo Transport." *Nano Letters* 24: 9129–9136. https://doi.org/10.1021/acs.nanolett.4c00209.

Nassir, N., M. A. Hashmi, K. G. Raji, et al. 2025. "Quantum Computing and the Implementation of Precision Medicine." *NPJ Genomic Medicine* 10: 80. https://doi.org/10.1038/s41525-025-00537-w.

Nedelec, F. 2002. "Computer Simulations Reveal Motor Properties Generating Stable Antiparallel Microtubule Interactions." *Journal of Cell Biology* 158: 1005–1015. https://doi.org/10.1083/jcb.200202051.

Nedelec, F., and D. Foethke. 2007. "Collective Langevin Dynamics of Flexible Cytoskeletal Fibers." *New Journal of Physics* 9: 427. https://doi.org/10.1088/1367-2630/9/11/427.

Ni, H., Q. Ni, G. A. Papoian, A. Trache, and Y. Jiang. 2023. "Myosin and [Formula: See Text]-Actinin Regulation of Stress Fiber Contractility Under Tensile Stress." *Scientific Reports* 13: 8662. https://doi.org/10.1038/s41598-023-35675-7.

Ni, Q., K. Wagh, A. Pathni, et al. 2022. "A Tug of War Between Filament Treadmilling and Myosin Induced Contractility Generates Actin Rings." *eLife* 11: e82658. https://doi.org/10.7554/eLife.82658.

Nordenfelt, P., H. L. Elliott, and T. A. Springer. 2016. "Coordinated Integrin Activation by Actin-Dependent Force During T-Cell Migration." *Nature Communications* 7: 13119. https://doi.org/10.1038/ncomms13119.

Oostenbrink, C., A. Villa, A. E. Mark, and W. F. van Gunsteren. 2004. "A Biomolecular Force Field Based on the Free Enthalpy of Hydration and Solvation: The GROMOS Force-Field Parameter Sets 53A5 and 53A6." *Journal of Computational Chemistry* 25: 1656–1676. https://doi.org/10.1002/jcc.20090.

Oosterheert, W., F. E. C. Blanc, A. Roy, et al. 2023. "Molecular Mechanisms of Inorganic-Phosphate Release From the Core and Barbed End of Actin Filaments." *Nature Structural and Molecular Biology* 30: 1774–1785. https://doi.org/10.1038/s41594-023-01101-9.

Owen, L. M., N. A. Bax, W. I. Weis, and A. R. Dunn. 2022. "The C-Terminal Actin-Binding Domain of Talin Forms an Asymmetric Catch Bond With F-Actin." *Proceedings of the National Academy of Sciences of the United States of America* 119: e2109329119. https://doi.org/10.1073/pnas.2109329119.

Parsons, J. T., A. R. Horwitz, and M. A. Schwartz. 2010. "Cell Adhesion: Integrating Cytoskeletal Dynamics and Cellular Tension." *Nature Reviews. Molecular Cell Biology* 11: 633–643. https://doi.org/10.1038/nrm2957.

Paul, D. M., J. Mantell, U. Borucu, et al. 2020. "In Situ Cryo-Electron Tomography Reveals Filamentous Actin Within the Microtubule Lumen." *Journal of Cell Biology* 219: e201911154. https://doi.org/10.1083/jcb.201911154.

Peña Ccoa, W. J., F. Mukadum, A. Ramon, G. Stirnemann, and G. M. Hocky. 2025. "A Direct Computational Assessment of Vinculin–Actin Unbinding Kinetics Reveals Catch-Bonding Behavior." *Proceedings of the National Academy of Sciences* 122: e2425982122. https://doi.org/10.1073/pnas.2425982122.

Peng, Y., A. J. Pak, A. E. P. Durumeric, et al. 2023. "OpenMSCG: A Software Tool for Bottom-Up Coarse-Graining." *Journal of Physical Chemistry. B* 127: 8537–8550. https://doi.org/10.1021/acs.jpcb.3c04473.

Phillips, J. C., R. Braun, W. Wang, et al. 2005. "Scalable Molecular Dynamics With NAMD." *Journal of Computational Chemistry* 26: 1781–1802. https://doi.org/10.1002/jcc.20289.

Plattner, N., S. Doerr, G. De Fabritiis, and F. Noe. 2017. "Complete Protein-Protein Association Kinetics in Atomic Detail Revealed by Molecular Dynamics Simulations and Markov Modelling." *Nature Chemistry* 9: 1005–1011. https://doi.org/10.1038/nchem.2785.

Popov, K., J. Komianos, and G. A. Papoian. 2016. "MEDYAN: Mechanochemical Simulations of Contraction and Polarity Alignment in Actomyosin Networks." *PLoS Computational Biology* 12: e1004877. https://doi.org/10.1371/journal.pcbi.1004877.

Proctor, E. A., and N. V. Dokholyan. 2016. "Applications of Discrete Molecular Dynamics in Biology and Medicine." *Current Opinion in Structural Biology* 37: 9–13. https://doi.org/10.1016/j.sbi.2015.11.001.

Pulido Cifuentes, L. P. C., A. I. M. Athamneh, Y. Efremov, et al. 2024. "A Modified Motor-Clutch Model Reveals That Neuronal Growth Cones Respond Faster to Soft Substrates." *Molecular Biology of the Cell* 35: ar47. https://doi.org/10.1091/mbc.E23-09-0364.

Robinson, R. C., T. Chongrungreang, K. Ponlachantra, et al. 2025. "The Structure of an Actin Nucleus Stabilized by Villin." *Science Advances* 11: eadw6915. https://doi.org/10.1126/sciadv.adw6915.

Sahoo, A., and S. M. Hanson. 2025. "Microtubules in Martini: Parameterizing a Heterogeneous Elastic-Network Towards a Mechanically Accurate Microtubule." *PNAS Nexus* 4: pgaf202. https://doi.org/10.1093/pnasnexus/pgaf202.

Schaedel, L., S. Triclin, D. Chrétien, et al. 2019. "Lattice Defects Induce Microtubule Self-Renewal." *Nature Physics* 15: 830–838. https://doi.org/10.1038/s41567-019-0542-4.

19493592, 0, Downloaded from https://onlinelibrary.wiley.com/doi/10.1002/cm.70221, Wiley Online Library on [25/11/2026]. See the Terms and Conditions (https://onlinelibrary.wiley.com/terms-and-conditions) on Wiley Online Library for rules of use; OA articles are governed by the applicable Creative Commons License

Schmitt, M. S., J. Colen, S. Sala, et al. 2024. "Machine Learning Interpretable Models of Cell Mechanics From Protein Images." *Cell* 187: 481–494.e424. https://doi.org/10.1016/j.cell.2023.11.041.

Selvaraj, A. A., M. Jayawant, N. Kayalvizhi, et al. 2026. "Exploring Quantum Frontiers in Protein Structure Prediction: Techniques, Challenges, and Opportunities." *Methods* 251: 94–112. https://doi.org/10.1016/j.ymeth.2026.04.006.

Sens, P. 2020. "Stick-Slip Model for Actin-Driven Cell Protrusions, Cell Polarization, and Crawling." *Proceedings of the National Academy of Sciences of the United States of America* 117: 24670–24678. https://doi.org/10.1073/pnas.2011785117.

Sept, D., and F. C. MacKintosh. 2010. "Microtubule Elasticity: Connecting All-Atom Simulations With Continuum Mechanics." *Physical Review Letters* 104: 018101. https://doi.org/10.1103/PhysRevLett.104.018101.

Shamloo, A., and B. Mehrafrooz. 2018. "Nanomechanics of Actin Filament: A Molecular Dynamics Simulation." *Cytoskeleton (Hoboken)* 75: 118–130. https://doi.org/10.1002/cm.21429.

Shell, M. S. 2008. "The Relative Entropy Is Fundamental to Multiscale and Inverse Thermodynamic Problems." *Journal of Chemical Physics* 129: 144108. https://doi.org/10.1063/1.2992060.

Shigematsu, H., T. Imasaki, C. Doki, et al. 2018. "Structural Insight Into Microtubule Stabilization and Kinesin Inhibition by Tau Family MAPs." *Journal of Cell Biology* 217: 4155–4163. https://doi.org/10.1083/jcb.201711182.

Shmilovich, K., M. Stieffenhofer, N. E. Charron, and M. Hoffmann. 2022. "Temporally Coherent Backmapping of Molecular Trajectories From Coarse-Grained to Atomistic Resolution." *Journal of Physical Chemistry. A* 126: 9124–9139. https://doi.org/10.1021/acs.jpca.2c07716.

Sidky, H., W. Chen, and A. L. Ferguson. 2020. "Machine Learning for Collective Variable Discovery and Enhanced Sampling in Biomolecular Simulation." *Molecular Physics* 118: e1737742. https://doi.org/10.1080/00268976.2020.1737742.

Singh, Y., G. M. Hocky, and B. J. Nolen. 2023. "Molecular Dynamics Simulations Support a Multistep Pathway for Activation of Branched Actin Filament Nucleation by Arp2/3 Complex." *Journal of Biological Chemistry* 299: 105169. https://doi.org/10.1016/j.jbc.2023.105169.

Skora, T., J. Wu, D. Beckett, W. Xue, G. A. Voth, and T. C. Bidone. 2025. "On the Curvature and Relaxation of Microtubule Plus-End Tips." *Biophysical Journal* 125: 406–419. https://doi.org/10.1016/j.bpj.2025.07.003.

Souza, P. C. T., R. Alessandri, J. Barnoud, et al. 2021. "Martini 3: A General Purpose Force Field for Coarse-Grained Molecular Dynamics." *Nature Methods* 18: 382–388. https://doi.org/10.1038/s41592-021-01098-3.

Souza, P. C. T., L. Borges-Araújo, C. Brasnett, et al. 2025. "GoMartini 3: From Large Conformational Changes in Proteins to Environmental Bias Corrections." *Nature Communications* 16: 4051. https://doi.org/10.1038/s41467-025-58719-0.

Spiliotis, E. T., and K. Nakos. 2021. "Cellular Functions of Actin- and Microtubule-Associated Septins." *Current Biology* 31: R651–R666. https://doi.org/10.1016/j.cub.2021.03.064.

Sridharan Iyer, S., K. M. Herman, T. Paul, Y. Wang, T. D. Pollard, and G. A. Voth. 2025. "Reaching the Full Potential of Cryo-EM Reconstructions With Molecular Dynamics Simulations at 310 K: Actin Filaments as an Example." *Proceedings of the National Academy of Sciences of the United States of America* 122: e2521421122. https://doi.org/10.1073/pnas.2521421122.

Sridharan Iyer, S., J. Wu, T. D. Pollard, and G. A. Voth. 2025. "Molecular Mechanism of Arp2/3 Complex Activation by Nucleation-Promoting Factors and an Actin Monomer." *Proceedings of the National Academy of Sciences of the United States of America* 122: e2421467122. https://doi.org/10.1073/pnas.2421467122.

Stehbens, S., and T. Wittmann. 2012. "Targeting and Transport: How Microtubules Control Focal Adhesion Dynamics." *Journal of Cell Biology* 198: 481–489. https://doi.org/10.1083/jcb.201206050.

Suh, D., A. R. Arattu Thodika, S. Kim, K. Nam, and W. Im. 2024. "CHARMM-GUI QM/MM Interfacer for a Quantum Mechanical and Molecular Mechanical (QM/MM) Simulation Setup: 1. Semiempirical Methods." *Journal of Chemical Theory and Computation* 20: 5337–5351. https://doi.org/10.1021/acs.jctc.4c00439.

Sun, S., C. Karki, Y. Xie, et al. 2021. "Hybrid Method for Representing Ions in Implicit Solvation Calculations." *Computational and Structural Biotechnology Journal* 19: 801–811. https://doi.org/10.1016/j.csbj.2021.01.020.

Sun, S., H. Xu, Y. Xie, et al. 2023. "HIT-2: Implementing Machine Learning Algorithms to Treat Bound Ions in Biomolecules." *Computational and Structural Biotechnology Journal* 21: 1383–1389. https://doi.org/10.1016/j.csbj.2023.02.013.

Suozzi, K. C., X. Wu, and E. Fuchs. 2012. "Spectraplakins: Master Orchestrators of Cytoskeletal Dynamics." *Journal of Cell Biology* 197: 465–475. https://doi.org/10.1083/jcb.201112034.

Suter, D. M., and P. Forscher. 2001. "Transmission of Growth Cone Traction Force Through apCAM-Cytoskeletal Linkages Is Regulated by Src Family Tyrosine Kinase Activity." *Journal of Cell Biology* 155: 427–438. https://doi.org/10.1083/jcb.200107063.

Szczuka, M., G. P. Pereira, L. J. Walter, et al. 2026. "Fast Parametrization of Martini3 Models for Fragments and Small Molecules." *Journal of Chemical Theory and Computation* 22: 610–623. https://doi.org/10.1021/acs.jctc.5c01178.

Tai, L., G. Yin, X. Huang, F. Sun, and Y. Zhu. 2023. "In-Cell Structural Insight Into the Stability of Sperm Microtubule Doublet." *Cell Discovery* 9: 116. https://doi.org/10.1038/s41421-023-00606-3.

Thomasen, F. E., F. Pesce, M. A. Roesgaard, G. Tesei, and K. Lindorff-Larsen. 2023. "Correction to "Improving Martini 3 for Disordered and Multidomain Proteins"." *Journal of Chemical Theory and Computation* 19: 3022–3023. https://doi.org/10.1021/acs.jctc.3c00425.

Thomasen, F. E., T. Skaalum, A. Kumar, S. Srinivasan, S. Vanni, and K. Lindorff-Larsen. 2024. "Rescaling Protein-Protein Interactions Improves Martini 3 for Flexible Proteins in Solution." *Nature Communications* 15: 6645. https://doi.org/10.1038/s41467-024-50647-9.

Thompson, A. P., H. M. Aktulga, R. Berger, et al. 2022. "LAMMPS—A Flexible Simulation Tool for Particle-Based Materials Modeling at the Atomic, Meso, and Continuum Scales." *Computer Physics Communications* 271: 108171. https://doi.org/10.1016/j.cpc.2021.108171.

Ti, S. C., G. M. Alushin, and T. M. Kapoor. 2018. "Human Beta-Tubulin Isotypes Can Regulate Microtubule Protofilament Number and Stability." *Developmental Cell* 47: 175–190.e175. https://doi.org/10.1016/j.devcel.2018.08.014.

Tong, D., and G. A. Voth. 2020. "Microtubule Simulations Provide Insight Into the Molecular Mechanism Underlying Dynamic Instability." *Biophysical Journal* 118: 2938–2951. https://doi.org/10.1016/j.bpj.2020.04.028.

Torrie, G. M., and J. P. Valleau. 1977. "Nonphysical Sampling Distributions in Monte Carlo Free-Energy Estimation: Umbrella Sampling." *Journal of Computational Physics* 23: 187–199. https://doi.org/10.1016/0021-9991(77)90121-8.

Tsuji, C., M. Bradshaw, M. F. Allen, et al. 2024. "Author Correction: Cryoet Reveals Actin Filaments Within Platelet Microtubules." *Nature Communications* 15: 10328. https://doi.org/10.1038/s41467-024-54642-y.

19493592, 0, Downloaded from https://onlinelibrary.wiley.com/doi/10.1002/cm.70221, Wiley Online Library on [25/11/2026]. See the Terms and Conditions (https://onlinelibrary.wiley.com/terms-and-conditions) on Wiley Online Library for rules of use; OA articles are governed by the applicable Creative Commons License

Van Der Spoel, D., E. Lindahl, B. Hess, et al. 2005. "GROMACS: Fast, Flexible, and Free." *Journal of Computational Chemistry* 26: 1701–1718. https://doi.org/10.1002/jcc.20291.

Ventura Santos, C., S. L. Rogers, and A. P. Carter. 2023. "CryoET Shows Cofilactin Filaments Inside the Microtubule Lumen." *EMBO Reports* 24: e57264. https://doi.org/10.15252/embr.202357264.

Venturini, C., and P. Saez. 2023. "A Multi-Scale Clutch Model for Adhesion Complex Mechanics." *PLoS Computational Biology* 19: e1011250. https://doi.org/10.1371/journal.pcbi.1011250.

Vickery, O. N., and P. J. Stansfeld. 2021. "CG2AT2: An Enhanced Fragment-Based Approach for Serial Multi-Scale Molecular Dynamics Simulations." *Journal of Chemical Theory and Computation* 17: 6472–6482. https://doi.org/10.1021/acs.jctc.1c00295.

Waltmann, C., Y. Wang, C. Yang, S. Kim, and G. A. Voth. 2025. "MSBack: Multiscale Backmapping of Highly Coarse-Grained Proteins Using Constrained Diffusion." *Journal of Chemical Theory and Computation* 21: 6184–6193. https://doi.org/10.1021/acs.jctc.5c00459.

Wang, L., C. Brasnett, L. Borges-Araujo, P. C. T. Souza, and S. J. Marrink. 2025. "Martini3-IDP: Improved Martini 3 Force Field for Disordered Proteins." *Nature Communications* 16: 2874. https://doi.org/10.1038/s41467-025-58199-2.

Wang, Y., J. Wu, V. Zsolnay, T. D. Pollard, and G. A. Voth. 2024. "Mechanism of Phosphate Release From Actin Filaments." *Proceedings of the National Academy of Sciences of the United States of America* 121: e2408156121. https://doi.org/10.1073/pnas.2408156121.

Wehrle-Haller, B., and B. A. Imhof. 2003. "Actin, Microtubules and Focal Adhesion Dynamics During Cell Migration." *International Journal of Biochemistry and Cell Biology* 35: 39–50. https://doi.org/10.1016/S1357-2725(02)00071-7.

Wells, D. B., and A. Aksimentiev. 2010. "Mechanical Properties of a Complete Microtubule Revealed Through Molecular Dynamics Simulation." *Biophysical Journal* 99: 629–637. https://doi.org/10.1016/j.bpj.2010.04.038.

Williams, M. R., J. C. Tardiff, and S. D. Schwartz. 2018. "Mechanism of Cardiac Tropomyosin Transitions on Filamentous Actin as Revealed by All-Atom Steered Molecular Dynamics Simulations." *Journal of Physical Chemistry Letters* 9: 3301–3306. https://doi.org/10.1021/acs.jpclett.8b00958.

Winkelman, J. D., C. G. Bilancia, M. Peifer, and D. R. Kovar. 2014. "Ena/VASP Enabled Is a Highly Processive Actin Polymerase Tailored to Self-Assemble Parallel-Bundled F-Actin Networks With Fascin." *Proceedings of the National Academy of Sciences of the United States of America* 111: 4121–4126. https://doi.org/10.1073/pnas.1322093111.

Wriggers, W., and K. Schulten. 1999. "Investigating a Back Door Mechanism of Actin Phosphate Release by Steered Molecular Dynamics." *Proteins* 35: 262–273. https://doi.org/10.1002/(SICI)1097-0134(19990501)35:2<262::AID-PROT11>3.0.CO;2-N.

Wu, J., S. Dasetty, D. Beckett, et al. 2025. "Data-Driven Equation-Free Dynamics Applied to Many-Protein Complexes: The Microtubule Tip Relaxation." *Biophysical Journal* 124: 3853–3866. https://doi.org/10.1016/j.bpj.2025.01.009.

Wu, X., D. Li, Y. Chen, et al. 2024. "Fascin - F-Actin Interaction Studied by Molecular Dynamics Simulation and Protein Network Analysis." *Journal of Biomolecular Structure and Dynamics* 42: 435–444. https://doi.org/10.1080/07391102.2023.2199083.

Xue, W., J. Wu, T. Bidone, and G. A. Voth. 2026. "Lattice Instability Drives Formation of Protofilament Clusters at the Microtubule Plus-End Tips." *Biophysical Journal* 125: 1516–1531. https://doi.org/10.1016/j.bpj.2026.02.013.

Yang, S. K., S. Kubo, C. S. Black, et al. 2024. "Effect of Alpha-Tubulin Acetylation on the Doublet Microtubule Structure." *eLife* 12: RP92219. https://doi.org/10.7554/eLife.92219.

Zhang, R., G. M. Alushin, A. Brown, and E. Nogales. 2015. "Mechanistic Origin of Microtubule Dynamic Instability and Its Modulation by EB Proteins." *Cell* 162: 849–859. https://doi.org/10.1016/j.cell.2015.07.012.

Zhang, Z., L. Lu, W. G. Noid, V. Krishna, J. Pfaendtner, and G. A. Voth. 2008. "A Systematic Methodology for Defining Coarse-Grained Sites in Large Biomolecules." *Biophysical Journal* 95: 5073–5083. https://doi.org/10.1529/biophysj.108.139626.

Zhu, K., E. Trizio, J. Zhang, et al. 2025. "Enhanced Sampling in the Age of Machine Learning: Algorithms and Applications." *Chemical Reviews* 126: 671–713. https://doi.org/10.1021/acs.chemrev.5c00700.

Zhu, R., Y. Zhang, T. Zhu, and F. Xia. 2025. "Coarse-Grained Simulation of Persistence Length and Twisting Dynamics of Micrometer-Scale Microtubules." *Journal of Physical Chemistry Letters* 16: 7300–7306. https://doi.org/10.1021/acs.jpclett.5c01226.

Zsolnay, V., M. L. Gardel, D. R. Kovar, and G. A. Voth. 2024. "Cracked Actin Filaments as Mechanosensitive Receptors." *Biophysical Journal* 123: 3283–3294. https://doi.org/10.1016/j.bpj.2024.06.014.

Zuk, P. J., B. Cichocki, and P. Szymczak. 2018. "GRPY: An Accurate Bead Method for Calculation of Hydrodynamic Properties of Rigid Biomacromolecules." *Biophysical Journal* 115: 782–800. https://doi.org/10.1016/j.bpj.2018.07.015.

19493592, 0, Downloaded from https://onlinelibrary.wiley.com/doi/10.1002/cm.70221, Wiley Online Library on [25/11/2026]. See the Terms and Conditions (https://onlinelibrary.wiley.com/terms-and-conditions) on Wiley Online Library for rules of use; OA articles are governed by the applicable Creative Commons License